Journal of Environmental Chemical Engineering 10 (2022) 107969

Contents lists available at ScienceDirect

Journal of Environmental Chemical Engineering

journal homepage: www.elsevier.com/locate/jece

Solar-photovoltaic electrocoagulation of wastewater from a chocolate manufacturing industry: Anodic material effect (aluminium, copper and zinc) and life cycle assessment

Violeta Maricruz García-Orozco [a], Ivonne Linares-Hernández [b], Reyna Natividad [a], Patricia Balderas-Hernández [a], Claudia Alanis-Ramírez [a], Carlos E. Barrera-Díaz [a], Gabriela Roa-Morales [a,*]

[a] Centro Conjunto de Investigación en Química Sustentable UAEM-UNAM, Universidad Autónoma del Estado de México, Carretera Toluca-Atlacomulco, Km 14.5, Campus San Cayetano, 50200 Toluca, MEX, Mexico
[b] Instituto Interamericano de Tecnología y Ciencias de Agua (IITCA), Universidad Autónoma del Estado de México, Km.14.5, Carretera Toluca-Atlacomulco, C.P 50200 Toluca, Estado de México, Mexico

ARTICLE INFO

Editor: Vítor Jorge Vilar

Keywords:
Chocolate industry wastewater
Electrocoagulation
Zinc anode
Aluminium anode
Copper anode
Solar-photovoltaic

ABSTRACT

Wastewater from a chocolate industry with an acid pH (4.38), and a high content of organic matter (Chemical oxygen demand (COD) = 9566 mg/L), Biochemical oxygen demand (BOD_5) of 4666.97 mg/L, biodegradability index (BI) of 0.49 and Total organic carbon (TOC) of 1318.7 mg/L, was treated by solar-photovoltaic electrocoagulation. The effects of anodic material (aluminium, copper or zinc), pH (4.38 and 7) and current density (1.781 mA/cm^2 and 0.356 mA/cm^2) at 60 min of treatment time were studied. The aluminium system exhibited the best results: 50% and 39% removal efficiency of COD and BOD, respectively. The BI increased considerably from 0.49 to 0.59 while TOC diminished only 26.65%. The copper-based cell also showed an acceptable behaviour in the organic removal that was: 43% COD, 53% BOD, 30.7% TOC and the BI was 0.4. The zinc-based system was slightly less efficient than copper and aluminium, where the removal achieved was: 39% COD, 30% BOD_5, and 19% TOC. The BI showed an increase to 0.56, improving the biodegradability of wastewater. The quantification and characterization of sludge was carried out using SEM and EDS. Fourier Transform Infrared Spectroscopy (FTIR spectra) proved the removal of organic and nitrogenous matter by the coagulant. Although costs associated with energy savings were estimated, the use of a solar panel, nevertheless, led to energy reductions. According to Life cycle assessment, the Cu anode provided the highest environmental impact and the use of Zn involved a lower effect in all categories, except for marine ecotoxicity, human non-carcinogenic toxicity and human health.

1. Introduction

Chocolate products are the most widespread desserts and snacks around the globe [1]. The water consumption in the chocolate process is around 11,372 L/kg for moulded chocolates, followed by bagged chocolates (10,484 L/kg). The chocolate manufacturing industry has been reported to have high contents of total solids (TS), oils, sulphates, chlorides, fluorides, phosphorous, total nitrogen, biochemical oxygen demand BOD_5, COD and surfactants [2], saturated fats, polyphenols, methylxanthines aldehydes, pyrroles, mixtures of phospholipids, ketones, aliphatic alcohols, liquid cocoa butter triglycerides, glycolipids, volatile compounds di- and tri-terpenes, sterols, furans and flavonoids [3–8].

Efficient wastewater treatment technologies include electrochemical methods, for example, electro-oxidation (EO), electro-flotation (EF) and electrocoagulation (EC) [9–11]. These technologies are environmentally friendly because they have a small footprint, are reliable, economic, consume less treatment time, display large volume handling capacity, do not need chemical additives and generate minimal sludge quantities.

EC is an effective technique to remove heavy metals [12–14], non-metals [15–19], anions [20–22] and organic compounds [23–25] from drinking water and wastewater. EC has attracted sizeable attention

* Corresponding author.
E-mail address: groam@uaemex.mx (G. Roa-Morales).

https://doi.org/10.1016/j.jece.2022.107969
Received 23 December 2021; Received in revised form 14 May 2022; Accepted 21 May 2022
Available online 24 May 2022

because of its growing enforcement to treat wastewater for different industries, like gelatine [26,27], the collagen of animal hide or bone [28], potato chips [29], starches [30], proteins, carbohydrates[31], vitamins [32], pectin, sugars [33], fermented products [34], pasta, cookies [35], baker's yeast [36], molasses [37], caramel pigment [38], almonds [39] and chocolate industry [40].

During the EC process, an applied electrical current makes sacrificial anodes dissolve, generating active coagulant compounds and electrolytic reactions happen at the electrode surfaces. Different metals have been tested as anodic material: aluminum [41–43], copper [44,45], iron [14,46,47], stainless steel [48], Platinum Coated Titanium [49] and zinc [11,50,51].

Few works have been reported specifically for the chocolate industry wastewater treatment [52–55]. Among these works, only two of them [40,56] are related to the treatment of this type of wastewater by EC. Such works, however, have left aside the assessment of different type of electrodes since they have been dedicated to the testing of only one type of electrodes (aluminum). In this context, a proper electrode material selection is important because it impacts the coagulant specie, and this affects the overall contaminants removal efficiency and also the overall process cost. There are within literature some studies that asses the effect of the anodic material albeit on the removal efficiency of toxic metallic ions [57], chemical oxygen demand (COD) of a palm oil mill effluent [33], of textile [58], paper industry wastewater [59], metal working fluid wastewater [60], and perfluorooctanoic acid [61]. Hussin et al., 2017 [51], for instance, demonstrated the superiority of zinc as sacrificial anode when compared with Cu, Fe and Al to remove Pb (II). The removal efficiency achieved with zinc was 97.5% while 74.1%, 81.1% and 84.2% was achieved with Cu, Fe and Al, respectively. These results highlight the importance of assessing the type of electrode material. In this sense, although Fe hydroxylated species are well known to be an efficient coagulant, its use is restrained by the inherent and inevitable increase in color [33].

In the EC, direct current is passed through an anode (sacrificial electrode), to generate metallic ions ($M^{n+}_{(aq)}$) (Eq. 1), then water reduction proceeds at the cathode to produce HO^- and H_2, as Eq. (2) shows [62]. This promotes the formation of polyhydroxides and polyhydroxy-metallic compounds ($M(OH)_{n(s)}$), depending on the pH and metal involved, as seen in Eq. (3) [63]. After that, the colloidal pollutants are removed by adsorption on the surface of the electrochemically produced coagulant, which at the end of treatment is separated from solution by flotation or sedimentation [64].

$$M_{(s)} \rightarrow M^{n+}_{(aq)} + ne^- \quad (1)$$

$$2H_2O + 2e^- \rightarrow 2HO^- + H_2 \quad (2)$$

In the bulk solution,

$$M^{n+}_{(aq)} + nHO^- \rightarrow M(\mathrm{OH})_{n(s)} \quad (3)$$

As above stated, electrochemical treatments need direct current to be carried out. Few years back, this represented one of the most important limitations of electrochemical treatments because of the ever-growing fossil fuel resource limitations that give off also ill-contributing greenhouse gas emissions [65,66]. Nowadays, however, solar energy can be a friendly alternative and represents a green option. In EC systems, different works report solar panels as a source of energy [51,67–79]. There are only few studies, however, where the use of a battery, PWM (Pulse Width Modulation) solar charge controller is documented. This controller helps to maintain a constant potential to protect the battery and the devices powered by the solar panel, from the fluctuations produced by solar energy changes, i.e. the controller aims to regulate the fluctuations current or voltage to energize the electrodes [80,81]. A PWM charge controller also allows the battery being fully charged in an optimal and stable way.

The use of solar energy instead of that from fossil fuels is important for the sustainability of the process. Also, in this context and for the sake of a decarbonized future, it is important to establish the environmental impact of a process. For such a purpose, Life Cycle Assessment (LCA) can be applied. This is a standardised methodology that can be carried out and the resulting environmental impacts are useful to set the ground for environmental improvements [82], to establish the sustainability of a process, and to make economic and political decisions. Despite the relevance of LCA, the literature on this regard and electrocoagulation is also scarce. The few related studies deal with the treatment of textile wastewater [58] and wastewater from a paper industry [59]. Both studies determine the environmental impacts of using as sacrificial anodes Fe or Al in an electrocoagulation process applied to different effluents. In the former case, Al was found as the anodic material with the lowest environmental impact, while Fe took this place when the treated effluent was that of a paper industry. Thus, from these studies, the importance of conducting a LCA for each electrocoagulation process can be inferred.

Because of the aforementioned, the key objective of this research was to study and compare the performance of the EC process to treat wastewater from a chocolate manufacturing industry, using zinc, aluminium, and copper electrodes energized by solar energy, and to assess the midpoint and endpoint environmental impacts of the process by applying life cycle assessment methodology. For such a purpose, batch experiments were performed for the treatment of real chocolate wastewater under various experimental conditions. The variables of interest in this research were pH, current densities (CDs), electrolysis time and electrode materials. The pH is important because depending on the medium (acid or alkaline) different species are formed and favor the coagulation and / or precipitation of different pollutants. Current density is important because it controls the dose of coagulant that is produced in the system and affects the % removal of contaminants. Electrolysis time affects energy consumption and cost when direct current is applied. The materials influence the removal efficiency, because of different species and complexes are formed in the process, the materials affect the cost of the system. A complete characterization was carried out before and after the EC process to understand the physical chemistry of water, evaluating also the energy consumption and produced sludge.

2. Materials and methods

2.1. Wastewater sample and characterization

Industrial wastewater samples were obtained from the effluent of a chocolate industry located in the State of México, México. Samples were taken without previous treatment. They were collected in plastic containers and stored at 4 °C for characterization and electrochemical treatments.

The physicochemical parameters were characterized according to Standard Methods Procedures [83]: chemical oxygen demand (COD), biological oxygen demand (BOD_5), total organic carbon (TOC), turbidity, colour, sulphates, pH, nitrites, nitrates, total nitrogen, total phosphorus, electric conductivity, total coliforms and faecal coliforms.

The physicochemical analysis was done once, using a control in each test. Electrochemical treatments were made by triplicate and error bars were included in the graphs.

The wastewater from the chocolate industry is transported by waterpipes to the wastewater treatment plant in our research institute. The sampling was done before entering the treatment plant. The wastewater samples were gathered in 20 L plastic containers and kept at 4 ∘C until analysis and treatment. It is worth clarifying that the taken samples corresponded to the final effluent of the chocolate manufacturing industry.

2.2. Electrocoagulation treatment

The EC treatment of a wastewater from a chocolate factory was studied using a cylindrical reactor at bench scale (1.220 L). The treatment was conducted under batch mode, with dimensions of 22.4 cm height and 7.5 cm diameter, with a maximum volumetric capacity of 2 L. A volume of 1.220 L was used at all experiments, which were conducted under continuous stirring. Rectangular electrodes of copper, zinc and aluminium, were assessed as anode/cathode plates, of dimensions: 19.5 cm × 2.4 cm, and providing an anodic area of 280.8 cm^2. The electrical current supplied was 0.1 and 0.5 A (*j* 1.781 mA/cm^2 and 0.356 mA/cm^2), powered by a solar panel, connected to a charge controller. The order of magnitude of the current densities was elected based on other works that successfully applied low current densities [17, 40]. Sodium sulfate was added to the sample to obtain a concentration of 0.004 M as support electrolyte to achieve 1.781 mA/cm^2 and to increase the electric conductivity of the sample from 624.7 μS/cm to 1658 μS/cm. The electric conductivity was measured with a Hach ION450 Conductivity Meter. Different aliquots were taken every 10 min per hour of treatment time. The working pHs were 4.38 (natural pH of the sample) and 7, this last one adjusted with a NaOH solution (7.5 M). The experimental setup is shown in Fig. 1.

2.3. Methods of analysis

Scanning Electron Microscopy coupled with EDS detector analysis were performed aided by a JEOL JSM-6400 (SEM) with backscattered electrons (BSE) (10–20 kV) detector, coupled to a FlexSEM, model SU 1000 (Hitachi) *Electronic Data Systems* (EDS) (at 20 kV) with Quantax 75/80 Bruker detector at 500x, HV:20 kV, WD:11.3–11.6 mm, Px:0.32 μm and 80 μm. This was used to know the elemental composition and morphological properties.

A Shimadzu IR affinity-1S Fourier Transform Infrared Spectrophotometer was used to identify the main functional groups of organic compounds in a range of 3999–399 cm^{-1}.

These analyses were carried out to characterize the sludge obtained from EC treatment, after drying at 105°C, during 24 h, aiming to establish the composition.

Chemical species distribution diagrams were analysed by MEDUSA program [84]. For this purpose, the calculation of the ionic strength (*I*) is necessary. This is proportional to the concentration of electrically charged species in solution and it was calculated with Eq. (4) [85]. For this calculation the data summarized in Table 1S (supplementary material) were used. As can be seen in Table 1S, the concentration of cations and anions ($N\text{-}NO_2^-$, $N\text{-}NO_3^-$, Cl^-, PO_4^{3-}, SO_4^{2-} Fe^{2+}, Ca^{2+}, K^+, Mg^{2+}, Al^{3+}, Cu^{2+}, Zn^{2+} Na^+ and SO_4^{2-}) was taken into account.

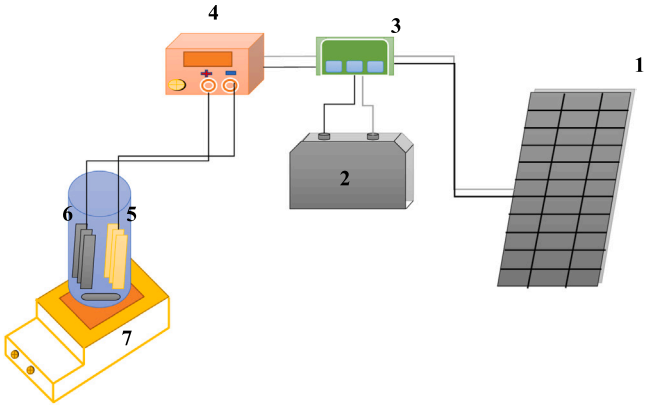

Fig. 1. Experimental set-up used for EC experiments: 1) Solar panel, 2) Deep cycle battery, 3) Solar charge controller, 4) Current controller, 5) Cathode, 6) Anode, 7) Magnetic stirrer.

$$I\left(mol\Big/L\right) = \frac{1}{2}\sum\left(C_i Z_i^2\right) \quad (4)$$

where Z_i is the charge of each ion and C_i is the concentration of each individual ion (mol/L).

2.4. Electrical cost and consumption

Cost and energy consumption of the EC was estimated considering the theoretical dissolution of the electrode material (*W*) calculated by the Faraday's law [86] as follows,

$$W\left(\frac{g}{L}\right) = \frac{itM}{nFv} \quad (5)$$

The electrical energy consumption *E* is defined by Eq. (6),

$$E\left(\frac{kWh}{L}\right) = \frac{Uit}{v} \quad (6)$$

where *i*, is current (A), *t* is time (s for Eq. 5), *M* is Al, Cu or Zn atomic weigh (g/mol), *v* is the sample volume (L), *F* is Faraday's constant (96,485 C/mol), *n* is the number of exchanged electrons during the anodic reaction, and it is 3 for Al and 2 for Cu and Zn, according to reaction 1, *U* is voltage (V) in Eq. (6).

The electricity cost in Mexico is US$ 0.040 per kWh [87]. The cost per liter of wastewater treated can be calculated with Eq. (7) [88],

$$\mathrm{Cos}\,t\left(\frac{US\$}{L}\right) = EC\left(\frac{kWh}{L}\right)(0.040) \quad (7)$$

2.5. Life cycle assessment (LCA)

The assessment conducted here followed the ISO 14044 guidelines [89,90] and included the following stages: goal and scope definition, functional unit (FU), system description and boundaries, life cycle inventory (LCI), impact assessment and interpretation. The goal was to assess the potential environmental impacts (mid and end point) of an electrocoagulation system for the treatment of wastewater from a chocolate factory under three scenarios of wastewater treatment that differ in the anodic material: scenario 1 (Zn), scenario 2 (Cu) and scenario 3 (Al). The scope of this study includes all values referred from cradle to grave, considering experimental data material and energy inputs, water emissions associated with the FU, the used reference flow was 1.220 L of treated water, with a volume allocation of 100% for its treatment.

The system boundary description (see Fig. 2) includes the electrochemical treatment of a wastewater chocolate factory according to Section 2.2. The LCI was established according with the experimental results obtained in this work at optimum conditions. To analyse and compare the impact categories, the software SimaPro® 9.1.0.11 PhD was used, developed by Pré Consultants. Inventory models for inputs were obtained from the Ecoinvent v.3 database. The environmental potential midpoint impacts were evaluated using ReCiPe 2016 Endpoint (H) V1.04 / World (2010) H/A [91]. This is an updated database and therefore is typically preferred to conduct LCA in the context of water treatment. The assessed midpoint impacts include 18 categories: global warming (GW) ($kgCO_{2eq}$), stratospheric ozone depletion (SOD) (kg CFC11 eq), ionizing radiation (IR) (kBq Co-60 eq), ozone formation, human health (OfHh) (kg NOx eq), fine particulate matter formation (FPmf) (kg PM 2.5 eq), ozone formation, terrestrial ecosystems (OfTe) (kg NOx eq), terrestrial acidification (TA) (kg SO2 eq), freshwater eutrophication (FE) (kg P eq), marine eutrophication (MA) (kg N eq), terrestrial ecotoxicity (TEc) (kg 1,4-DCB), freshwater ecotoxicity (FEc) (kg 1,4-DCB), marine ecotoxicity (MEc) (kg 1,4-DCB), human carcinogenic toxicity (HcT) (kg 1,4-DCB), human non-carcinogenic toxicity (HncT) (kg 1,4-DCB), land use (LU) (m^2a crop eq), mineral resource

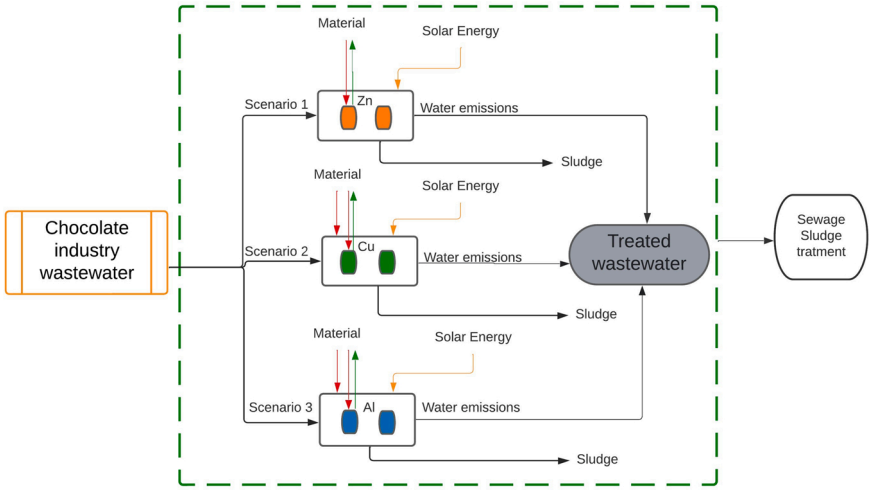

Fig. 2. System boundary for the treatment of wastewater from a chocolate factory with three anodic materials: scenario 1 (Zn), scenario 2 (Cu) and scenario 3 (Al).

scarcity (MRs) (kg Cu eq), fossil resource scarcity (FRs) (kg oil eq) and water consumption(WC) (m^3).

The impact factor scores, expressed in millipoints (mPts), of the end-point environmental indicators (Human Health Damage, Ecosystem Quality, and Resource Availability), for scenarios 1, 2 and 3 were calculated.

3. Results and discussion

3.1. Physicochemical characterization of industrial wastewater

Table 1 summarizes the results of the physicochemical characterization of the industrial wastewater prior treatment. The initial chocolate wastewater sample has an acid pH of 4.38, the content of organic matter was characterized by COD of 9566 mg/L, BOD_5 4666.97 mg/L. The biodegradability index (BI) was 0.49, according to Metcalf and Eddy [92] a wastewater with BI<0.5 is not easily biodegradable. The chocolate wastewater sample presents a BI slightly under this value. TOC was 1318.7 mg/L. This kind of wastewater sample from chocolate industry is characterized for the presence of high nitrogen and phosphorous contents. The sample contains 95 mg/L as total nitrogen, 11.7 mg/L N- NH_3 mg/L, 1.3 mg/L N-NO_3^- mg/L and 0.95 mg/L N-NO_2^- mg/L. On the same sample, 36.82 mg/L of PO_4^{3-} was detected. This N and P content is enough to cause problems associated with eutrophication including profuse algal blooms, excessive growth of nuisance aquatic plants, negative aesthetic aspects and deoxygenation [19]. The sample contains high colour and turbidity (891 Pt-Co units and 1082.67 NTU), the presence of chloride ions was detected (294.92 mg/L), so that it is possible that during electrochemical processes chlorine gas is formed, although this may help wastewater disinfection, since 1.6×10^6 MPN/100 mL of total and faecal coliforms were detected in the sample. Also, the metals: Al (0.48 mg/L), Cu (0.19 mg/L) and Zn (0.35 mg/L) were characterized. Additionally, monovalent and bivalent cations were determined in the sample.

Table 1 shows the final concentrations of Al, Cu and Zn after EC processes; however, because of the high metal concentration, the pH was increased to 9 so the ions concentration in the solution decreased. Both concentrations are reported in Table 1.

The parameters reported in Table 1 were chosen according to the Mexican standard NOM-002-SEMARNAT-1996.

Table 1
Chocolate wastewater characterization before and after EC treatments.

Parameter	Units	Initial	Final characterization		
			Cu	Al	Zn
pH	–	4.38	5.03	4.98	4.87
Colour	Pt-Co U	891	110	81	93
COD	mg/L	9566	5431	4808	5814
BOD_5	mg/L	4666.97	2173.04	2852.84	3245.31
BOD_5/COD		0.49	0.4	0.59	0.56
TOC	mg/L	1318.7	913.62	967.21	1069.37
Nitrites	N-NO_2^- mg/L	0.95	0.31	0	0.7
Nitrates	N-NO_3^- mg/L	1.3	1.3	0.6	0.7
Ammoniacal nitrogen	N- NH_3 mg/L	11.7	13.9	12.7	17.9
Total nitrogen	N mg/L	95	31	33	48
Phosphate	PO_4^{3-} mg/L	36.82	15.82	3.59	30.02
Turbidity	NTU	1082.67	88.9	19.2	283
Total dissolved solids	mg/L	1263	1539	1464	853
Total Suspended Solids	mg/L	1397	3	12	36
Total solids	mg/L	2660	1541	1476	889
Total coliforms	MPN/100 mL	1.6×10^6	< 200	< 200	< 200
Faecal coliforms	MPN/100 mL	1.6×10^6	< 200	< 200	< 200
Chlorides	Cl^- mg/L	294.92	225.89	158.96	192.42
Fe	mg/L	3.22	1.89	1.93	1.52
Ca	mg/L	167.39	24.55	18.22	18.73
K	mg/L	24.41	21.41	20.05	20.26
Mg	mg/L	12.35	11.37	4.13	9.93
Al	mg/L	0.48	0.19	106.4 3.14 (at pH 9)	0.24
Cu	mg/L	0.19	265.66 17.3 (at pH 9)	0.15	0.08
Zn	mg/L	0.35	0.25	0.29	198.6 2.66 (at pH 9)

3.2. Electrocoagulation treatment

3.2.1. pH effect

The initial pH is an important parameter in EC. It is worth noticing that pH increases during EC by the electrochemical reaction. This is generated by water reduction at the cathode to produce H_2 gas and HO^- ions [62].

Figs. 3, 4 and 5 show the pH effect on the COD removal at a current

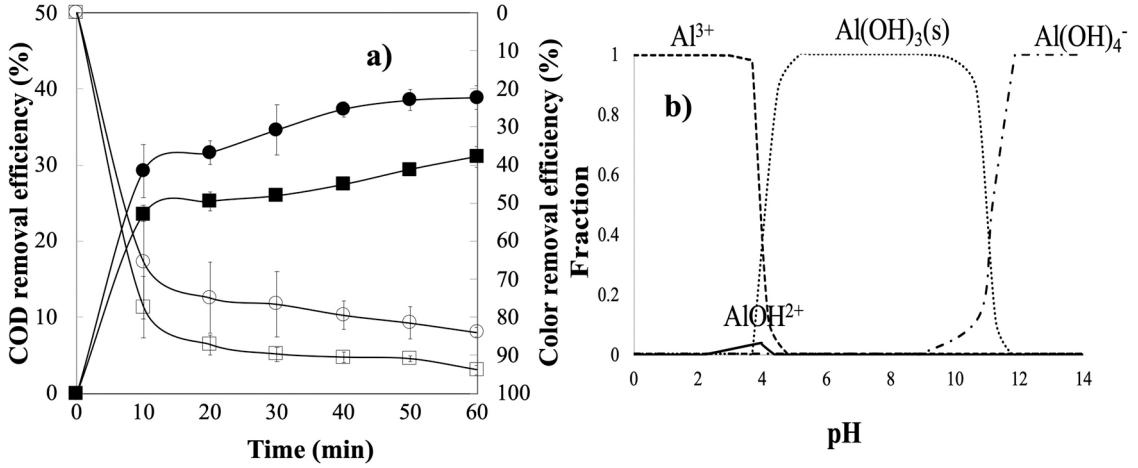

Fig. 3. Aluminium electrocoagulation performance: Effect of pH on the COD and Colour removal efficiency after 60 min of treatment and 0.356 mA/cm^2, **a)** pH 4.38 (•COD and ○ Colour) and pH 7 (■COD and □Colour) and b) Aluminium species distribution diagram in wastewater as a function of pH (I=0.02 and Al^{3+}=1.02 mM, NO_3^- = 20.97 μM, PO_4^{3-}= 0.39 mM, Cl^-= 8.32 mM, NO_2^-=20.65 μM).

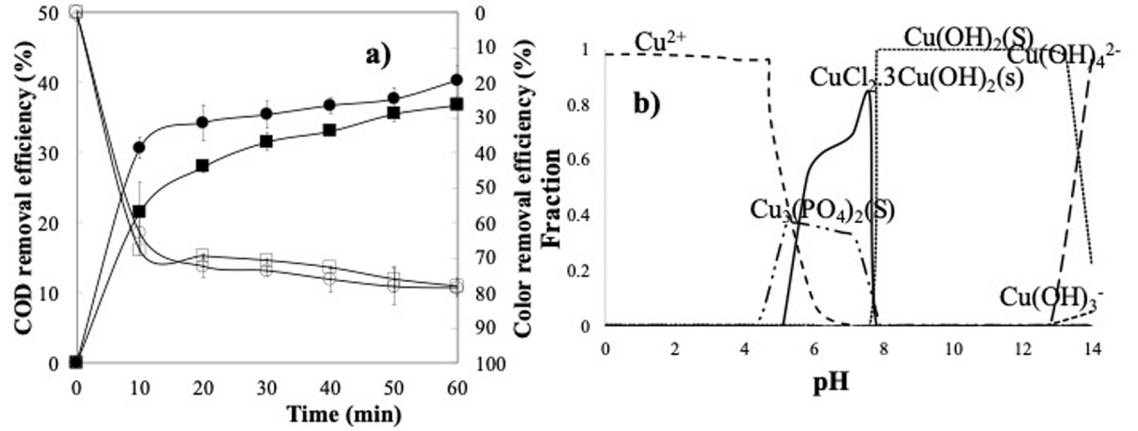

Fig. 4. Copper electrocoagulation system performance: Effect of pH on the COD and Colour removal at 60 min treatment and 0.356 mA/cm^2, **a)** pH 4.38 (•COD and ○ Colour) and pH 7 (■COD and □Colour) and b) Copper species distribution diagram in wastewater as a function of pH (I=0.02 and Cu^{2+}=1.53 mM, NO_3^- = 20.97 μM, PO_4^{3-}= 0.39 mM, Cl^-= 8.32 mM, NO_2^- =20.65 μM).

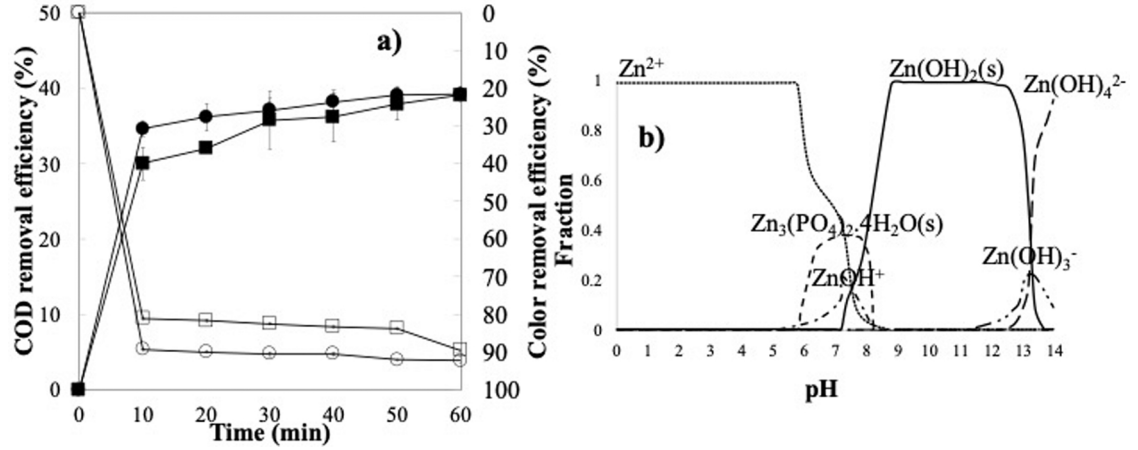

Fig. 5. Zinc electrocoagulation performance: Effect of pH on the COD and Colour removal at 60 min treatment and 0.356 mA/cm^2, **a)** pH 4.38 (•COD and ○ Colour) and pH 7 (■COD and □Colour) and **b)** Zinc species distribution diagram in wastewater as a function of pH (I=0.02 and Zn^{2+}=1.53 mM, NO_3^- = 20.97 μM, PO_4^{3-}= 0.39 mM, Cl^-= 8.32 mM, NO_2^-=20.65 μM).

density of 0.356 mA/cm^2, 1 h of treatment time and initial COD 9566 mg/L, colour 891 Pt-Co U, using Cu, Al and Zn as anodes in the electrolytic cell, pH of 4.38 (natural pH of the wastewater) and 7 (neutral pH) adjusted with sodium hydroxide.

Fig. 3a shows the aluminium electrocoagulation performance and the pH influence on the COD and colour removal. 31% of COD removal was achieved at initial pH 7 and 39% at pH of 4.38. At the same time, 80–90% of colour was removed in this treatment. During EC the pH increased to 4.98 and 7.30, respectively. According to aluminium species distribution diagram (Fig. 3b), $Al(OH)_3$ was produced in this pH range (Eq. 8) [93].

$$Al^{3+} + 3HO^- \rightarrow Al(OH)_3 \quad (8)$$

The pH evolution with time, exhibited by the copper EC system, is shown in Fig. 3. It can be observed that the natural pH sample increased from 4.38 to 5.03. One of the main species formed was Cu^{2+} [94] which favours the precipitation of phosphate ions in the chocolate wastewater as $Cu_3(PO_4)_{2(s)}$ [95] and $CuCl_2{\cdot}3Cu(OH)_2$ [96] (Eqs. 11–12). Eqs. 9–10 show the chemical reactions that occurred in the aqueous media. At neutral pH, the samples pH increased to 8.02 and $Cu(OH)_2$ (s) was formed at this pH [97]. The best removal of 37% COD and 80% of colour were achieved after 60 min of treatment time at an initial pH of 4.38.

In the EC process, different species contributed to destabilization of the organic and inorganic macromolecules by charge neutralization [98], these produce the agglomeration of neutral colloidal entities, promoting the flotation by hydrogen gas or precipitation by sedimentation [99].

$$Cu_{(s)} \rightarrow Cu^{2+}_{(aq)} + 2e^- \quad (9)$$

$$Cu_{(s)} + 2H_2O_{(l)} \rightarrow Cu(OH)_{2(s)} + H_{2(g)} \quad (10)$$

$$3Cu^{2+} + 2H_2PO_4^- \rightarrow Cu_3(PO_4)_{2(s)} + 4H^+ \quad (11)$$

$$2Cu_2O + 2HCl + 2H_2O + O_2 \rightarrow CuCl_2{\cdot}3Cu(OH)_{2(s)} \quad (12)$$

Further, the Zn system showed a pH increase from 4.38 to 4.87, while the neutral pH sample increased to 7.74. Fig. 5 shows the behaviour of COD and colour removal efficiency observed at these pHs in the Zn system. In both treatments, 39% of COD and 90% of colour were eliminated. Eq. (13) shows the anodic oxidation in the electrochemical cell, and Eqs. 14–16 show the chemical reactions occurring in solution [100–102]. This electrode material produced a smaller coagulant amount than Al or Cu, however, a good removal of COD was observed in this system.

$$Zn \rightarrow Zn^{2+} + 2e^- \quad (13)$$

$$Zn^{2+} + 2H_2O \rightarrow Zn(OH)_{2(s)} + 2H^+ \quad (14)$$

$$ZnO_{(s)} + H^+ \rightarrow ZnOH^+ \quad (15)$$

$$3Zn^{2+} + 2H_2PO_4^- + 4H_2O \rightarrow Zn_3(PO_4)_2.4H_2O + 4H^+ \quad (16)$$

$Al(OH)_3$ is characterized by its amphoteric character; it can react or behave as an acid or a base. $Al(OH)_3$ reacts with H_3O^+ ions to form the aqueous complex $[Al(OH_2)_6]^{3+}$ that hydrolyzes to acidify the medium, thus Al^{3+} is an acid ion; the working pH is 4.38 and according to the species distribution diagram, Al^{3+} is present at low concentration. However, $Al(OH)_3$ also behaves like a base, since it reacts with H_3O^+. On the other hand, it can react with HO^-, behaving as an acid forming Al $(OH)_4^-$, this complex is formed from pH 10, although this was not formed in the present work. Therefore $Al(OH)_3$ behaves as an electrocoagulant.

In the case of Cu and Zn, the $Cu(OH)_2$ and $Zn(OH)_2$ species are formed from pH 8, so they are not present during the EC process. The residual water from the chocolate industry is very stable due to the phosphate buffer, therefore the precipitation reactions of phosphate ions and the formation of complexes with nitrogenous matter are favored, which explains the amphoteric behavior.

3.3. Effect of current density

Current density (*j*) is one of the most significant parameters in the EC process [103]. This controls the anodic dissolution, bubble generation, flocs growth, the shift in pH, energy consumption during the treatment, electric conductivity and the quantity of solids generated [104].

Fig. 6 shows the behaviour and effect produced by the *j* at 1.781 mA/cm^2 and 0.356 mA/cm^2, using Al, Cu and Zn anodes, at natural pH of 4.38. It is well known that increasing *j*, improves the removal efficiency of organic and inorganic pollutants [105] because the anodic dissolution also increases. As we can see, Figs. 6a and b show that the best results were observed at *j* 1.781 mA/cm^2 with Al and Cu electrodes. The Al-based system presented the best performance with a removal of 50% COD and 91% color, while the Cu-based system showed a lower removal than aluminum, 44% COD and 88% color were achieved.

Fig. 6c shows the best removal efficiencies for the zinc system, 39%

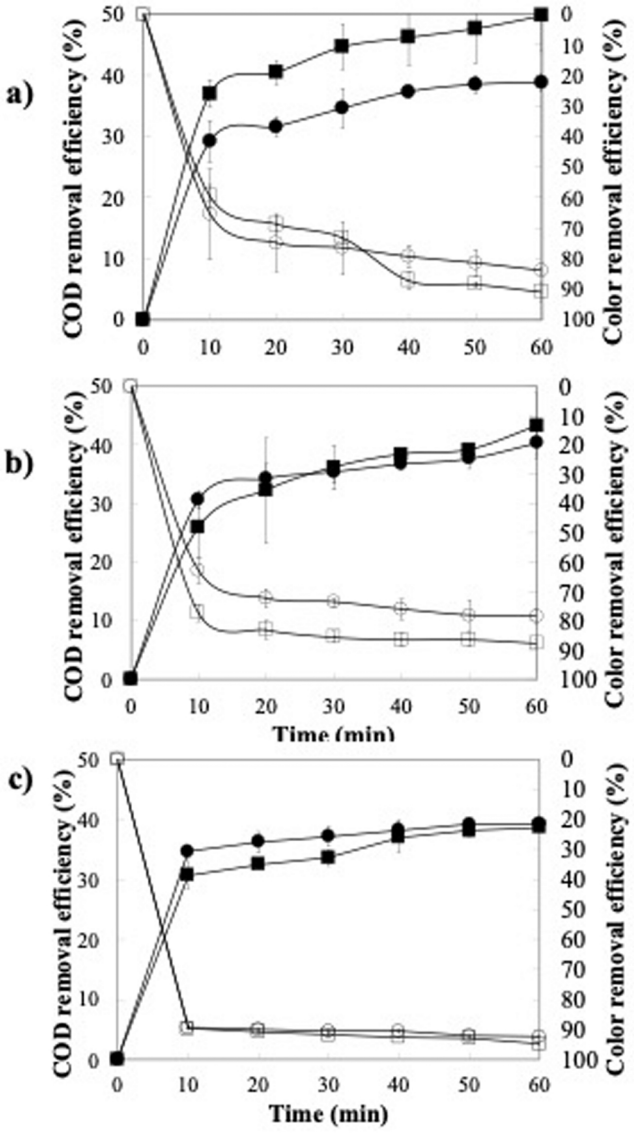

Fig. 6. Electrocoagulation performance: Effect of current density, *j*, on the COD and Colour removal at 60 min of treatment time and pH 4.38 a) aluminum system, b) Copper system; c) Zinc system. DQO (■1.781 mA/cm^2 and •0.356 mA/cm^2) and Color (□1.781 mA/cm^2 and ○0.356 mA/cm^2).

COD and 92% color removal were obtained at the smallest *j* (0.356 mA/cm^2).

In addition, it can be observed in Table 1, that the total dissolved solids increase with the EC that was carried out with Al and Cu electrodes. This is not observed in the case of the Zn electrodes, however, the total dissolved solids removal with this material is only 32%. The total dissolved solid concentrations in Table 1 are linked to the metallic ions that are detached from the sacrificial electrode and that were not used during the treatment and that did not precipitate.

This leads to a loss of anodic material. It is worth noticing that the total solids were removed in a 67%, 50% and 42% in the following order as function of anodic material: Zn>Al>Cu.

3.4. Kinetics

The kinetic data of the assessed treatments were analysed by applying basic power law models; however, a low correlation coefficient was obtained. Hence, the Behnajady-Modirshahla–Ghanbery model (BMG) was used. This model is obtained from the mathematical differentiation of a second order adsorption equation. This model recognizes two main steps dictating the removal rate of pollutants, i.e. the flocs production (Eq. 1) and then the adsorption of contaminants on them (Eq. 3). The BMG model is given by Eq. (17) [106],

$$C_t = \left(1 - \left[\frac{t}{m + bt}\right]\right) * C_0 \quad (17)$$

where C_t is the COD and color concentration at time *t*, the initial concentration of COD and color at time t = 0 min is C_0, *t* is the reaction time in min. 1/*m* is the COD or color removal rate at the beginning of the process and 1/*b* is the maximum theoretical fraction of removal [107].

Fig. 7 shows a) the COD removal and b) the color removal. The *m* and *b* constants are given in Table 2. These constants were calculated with the software Statistica 10 StatSoft®. The high correlation coefficients showed that the applied kinetic model displayed good correspondence with the data. BMG model represents well the experimental data because the EC occurred in two stages: coagulation occurred very fast during the first 10 min and then sedimentation occurred during the last 50 min Fig. 6a shows that COD removal is faster with Al Electrodes and Fig. 6b shows that after 40 min of treatment, the color removal is the same with the three different materials but at different reaction rates.

It can be observed in Table 2 that the smallest *m* corresponds to the Zn system. This means that Zn is the material that produces a faster initial removal rate of both, COD and color. Even so, constant *b* revealed that Al was the material producing a greater color and COD removal % at the end of the process.

3.5. UV-Vis spectroscopy

Fig. 9 shows the Uv-Vis spectra of the samples obtained at the best conditions for each treatment. The samples were diluted 1/20 for the analyses; turbidity, organic and inorganic matter were reduced considerably after treatments.

Aluminum is the material with the lowest absorbance in a range of 200–900 nm, after EC. This material removed all turbidity from the sample, but there is still organic matter seen at the 200–325 nm wavelength; the same spectrum is shown in this range as in the sample treated with Zinc electrodes. It is not known to which species this absorbance is related, but it is completely removed with the Copper electrodes. Thus, the increase in absorbance is due to the link of Copper with the organic matter of the medium.

Zinc and copper have the same absorbances of 325–900 nm, but Zinc has a turbidity three times greater than copper. This was reflected on the COD concentration.

3.6. Sludge Characterization

After EC treatment, the sludge was characterized by SEM and EDS. Fig. 10 shows the heterogeneous and irregular morphology of the a) Al, b) Cu and c) Zn sludge.

The analysed samples section showed the following elements in common C, O, Si, S, P, Fe, Mg and Al. The quantitative analysis indicates that the average mass (%) of chemical constituents of the sludge sample are: a) C 21.01%, O 56.97%, Na 0.39%, Mg 0.76%, Al 18.00%, Si 1.00%, S 1.02%, Ca 0.38% and P 0.13%, b) C 55.28%, O 37.08%, Si 0.44%, S 0.53%, Cu 5.23%, P 0.60%, Fe 0.51%, Mg 0.18% and Al 0.15%, and c) C 30.16%, O 28.83%, Mg 0.45%, Al 0.19%, Si 1.10%, P 0.67%, S 0.58%, Ca 0.81%, Fe 0.54%, Zn 31.34%, K 0.29% and Na 5.06%.

These elements are associated with the organic matter (carbon) and inorganic ions from chocolate wastewater, as well as the anodic metals that were removed after the EC process [108].

Fig. 11 depicts the FTIR spectrum which exhibits different bands in the 3000–3700 cm^{-1} range, assigned to the stretching vibration of O-H bonds of the different polymorphs of $Al(OH)_3$, $Cu(OH)_2$ and $Zn(OH)_2$ [109]. The peak at 1637–1647 cm^{-1} represents hydroxyl bending and γ′(OH) water bending vibration or overtones of hydroxyl bending [110]. Peaks at 2919–2921 and 2851–2855 cm^{-1}, correspond to the C-H stretching mode of saturated C-C bonds, showing the presence of hydrocarbons in the sludge [111], while the peak around 1051–1075 was assigned to carbonate mode. A stretching vibration of the Al-O bond at 554 cm^{-1} was also observed in the Al [112]. In addition, the presence of conjugated carbon–carbon bond is corroborated by a medium intensity band at 1464–1469 [113]. Peaks at 1745 in the Al, Cu systems and 1744 cm^{-1} in the Zn can be associated to stretching vibration of C═O [114].

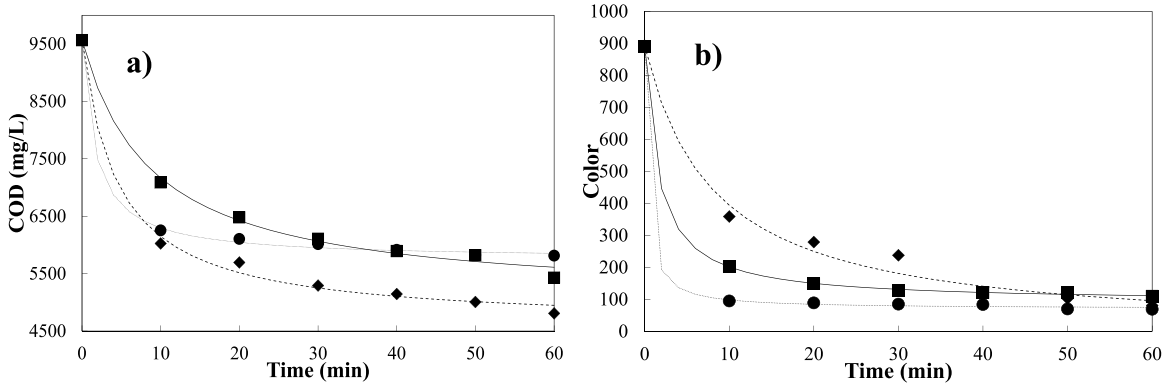

Fig. 7. Kinetic BGM modeling of the a) COD and b) colour removal; Al electrodes (◆), Cu electrodes (■) and Zn electrodes (•), Model Al (——), Model Zn (————), Model Cu (———).

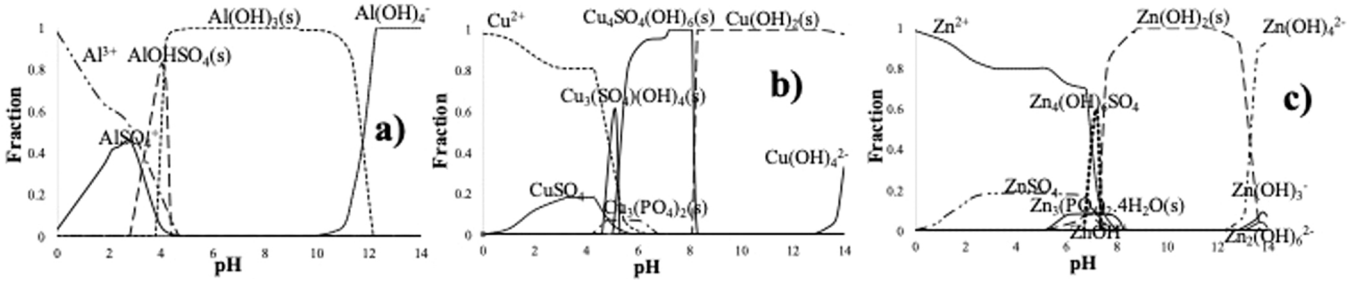

Fig. 8. Species distribution diagrams in wastewater as a function of pH at $j = 1.781$ mA/cm^2 with electrodes a) Al (Al^{3+}= 5.11 mM and I=0.058), b) Cu (Cu^{2+}= 7.65 mM and I=0.050) and c) Zn (Zn^{2+}= 7.65 mM and I=0.050).

Table 2
The coefficients of determination and characteristic constants of BMG.

Electrode material	Colour Removal			COD Removal		
	m (min)	*b*	r^2	*m* (min)	*B*	r^2
Al	8.070848	0.986366	0.98661708	8.700301	1.926605	0.9957448
Cu	1.781608	1.113641	0.999911	18.787766	2.105534	0.99517004
Zn	0.380186	1.085942	0.9996909	4.171368	2.507814	0.99879533

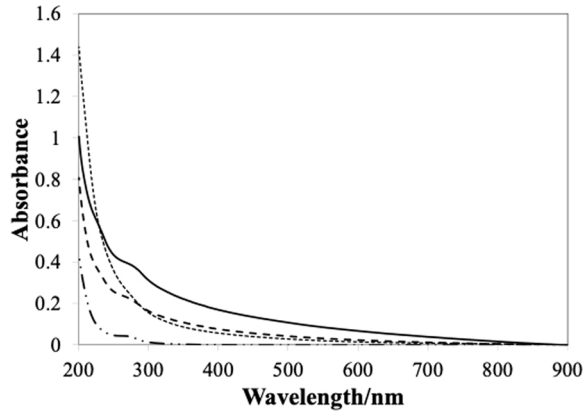

Fig. 9. Uv-Vis Spectra of Al 1.781 mA/cm^2, Cu 1.781 mA/cm^2 and Zn 0.356 mA/cm^2: Zn (——), Cu (————), Initial (———), Al (–··).

3.7. Physicochemical characterization of industrial wastewater after EC treatments

Table 1 shows the physicochemical characterization of the chocolate industry wastewater before and after EC for Cu, Al and Zn systems.

The aluminium-based system rendered the best results for organic and inorganic parameters: COD was reduced from 9566 mg/L to 4808 mg/L which represents a 50% removal and BOD was reduced from 4666.97 to 2852.84 mg/L, achieving 39% removal. The BI was increased considerably from 0.49 to 0.59. TOC diminished only 26.65% because EC does not mineralize organic matter. Color and turbidity were considerably improved: 90% and 98% were achieved, respectively. Both values, COD and color removal, were inferior to those observed at the same current density with Al electrodes albeit under a different hydrodynamics [40]. Such a study also deals with the treatment of wastewater from a chocolate manufacturing industry. A 63% and 97% of COD and color removal, respectively, was reported [40]. The differences can be ascribed to the different hydrodynamics and to the fact that in the previous study the initial COD was almost half (ca. 5000 mg/L) of that used in this manuscript (9566 mg/L). Compared to the results reported in [56], the achieved COD removal in this work (50%) is higher than that reported in a batch system also with Al electrodes [56]. This can be ascribed to the higher current density applied in this case. Regarding color, the removal of this parameter was higher (98.2%) at lower current densities [56] than the ones applied in this work.

Regarding total nitrogen (Table 1), it was reduced from 95 to 33 mg/L and ammoniacal nitrogen was slightly increased from 11.7 to 12.7 mg/L, final nitrates concentration (0.6 mg/L) and nitrites were not detected. Also, phosphate ions were 90% reduced. The electrochemical reduction of NO_3^- is reported by some authors to occur according with Eqs. 18 and 19 [115],

$$8e^- + NO^-_{3(aq)} + 10H^+_{(aq)} \rightarrow NH^+_{4(aq)} + 3H_2O_{(l)} \quad (18)$$

$$NH_4^+ + HO^- \leftrightarrow NH_3.H_2O \leftrightarrow NH_3 + H_2O \quad (19)$$

Cl^- ions were measured at the beginning and at the end of treatment, according with standard methods. Eqs. 20–22 describe the chlorine production at the anode and the hypochlorite formation in solution [17, 40]. The chlorine production is expected because after the EC treatment chloride ions concentration were diminished for Al, Cu, and Zn systems and an odor of chlorine was perceived during treatments. In addition, fecal and total coliforms were reduced significantly (99% reduction).

$$2Cl^- \rightarrow Cl_2 + 2e \quad (20)$$

$$Cl_2 + H_2O \rightarrow HClO + H^+ + Cl^- \quad (21)$$

$$HClO \rightarrow H^+ + ClO^- \quad (22)$$

For the Aluminium system, the final pH was 4.98 then the formation of $Al(OH)_{3(s)}$ observed in Fig. 7a), is expected.

The copper system was the second best in the organics removal. The obtained removal results with copper electrodes were: 43% COD, 53% BOD, 30.7% TOC and the BI was 0.4. Nitrogenous matter exhibits a similar behaviour than Al system. TN was reduced 67%, ammoniacal nitrogen was also increased from 11.7 to 13.9 mg/L, nitrates did not present any change and nitrites were reduced from 0.95 to 0.31 mg/L. According with Eq. (11) and Fig. 8, the phosphate precipitation was carried out in the Cu system as $Cu_3(PO_4)_2$, 57% removal was obtained. 87% color and 91.7% turbidity were achieved. In addition, 99% total and fecal coliforms were removed using Cu EC system due to Eqs. (20–22).

The three different materials at their best conditions show what can be used as pretreatment, because after 10 min, all the organic and inorganic suspended and colloidal matter was removed. After 30 min of treatment the removal of COD is practically constant, soluble COD

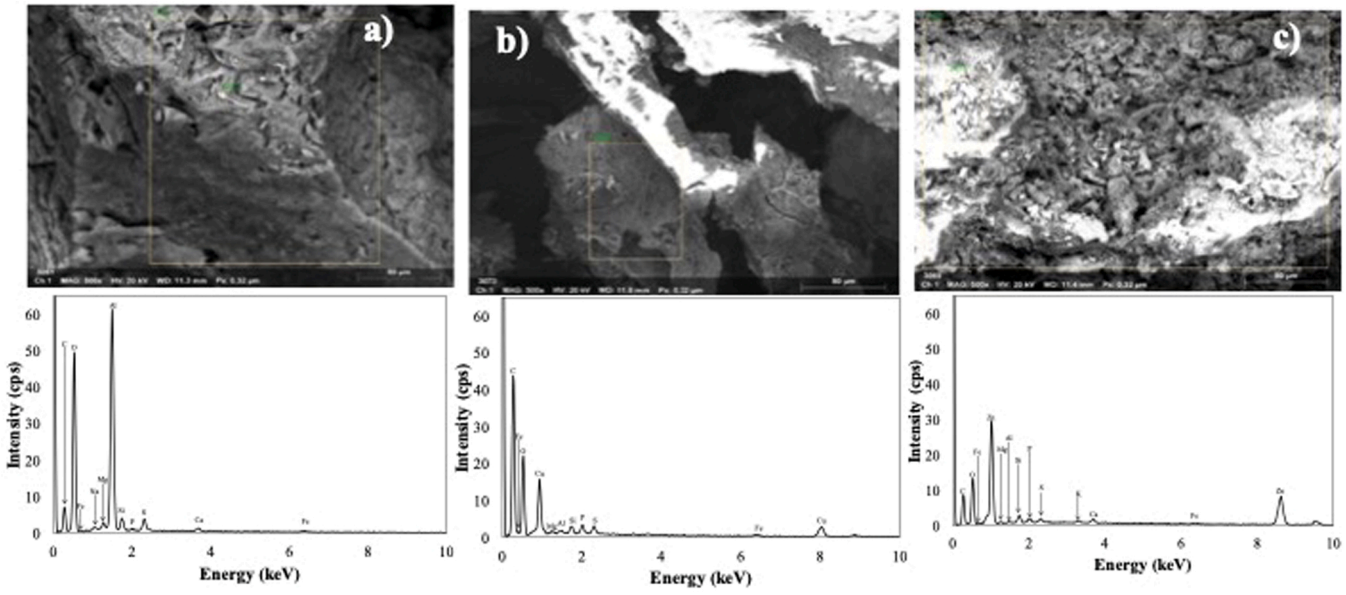

Fig. 10. SEM and EDS images of sludge generated during EC process with electrodes of a) Al, b) Cu and c) Zn.

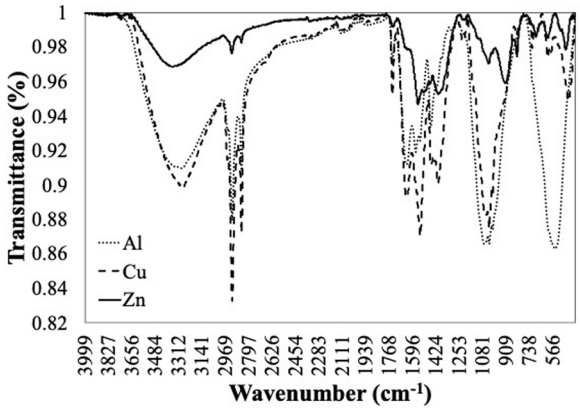

Fig. 11. FTIR spectra of sludge generated during EC process with electrodes of a) Al (·····), b) Zn(——) and c) Cu(———).

remains in the wastewater. Some recalcitrant characteristics (humic and fulvic acids) could be present in the wastewater, so that BOD_5 removal is also low.

Na_2SO_4 was added as supporting electrolyte, then Fig. 8 shows the species that are produced by adding SO_4^{2-} (6.59 mM). In the Cu system, the increase of pH was 5.03, then Cu^{2+}, $Cu_3(SO_4)(OH)_4$(s), $Cu_4SO_4(OH)_6$ (s) [116], $CuSO_4$ [117] and $Cu_3(PO_4)_2$(s) in Fig. 7b) could be formed, according with Eqs. (9,11) and (23–25).

$$Cu + SO_4^{2-} \rightarrow CuSO_4 \quad (23)$$

$$4Cu^{2+} + SO_4^{2-} + 6(HO)^- \rightarrow Cu_4SO_4(OH)_6 \quad (24)$$

$$3Cu^{2+} + 4HO^- + SO_4^{2-} \leftrightarrow Cu_3(SO_4)(OH)_4 \quad (25)$$

The zinc-based system was slightly less efficient than Cu and Al since the removal achieved was 39% COD (from 9566 to 5814 mg/L), 30% BOD_5 (from 4666 to 3245.31 mg/L), 19% TOC (1318.7–1069.37 mg/L). The BI shows an increase from 0.49 to 0.56, improving the biodegradability of wastewater. Color and turbidity presented a reduction of 89.5 mg/L and 73.86%, respectively. Total and fecal coliforms were reduced 99%. The reduction of TN was only 49% and this system achieved a higher formation of ammoniacal nitrogen (from 11.7 to 17.9 mg/L), nitrates and nitrites achieved a concentration of 0.7 mg/L (46% and 26% respectively). Phosphates were slightly diminished (18.46%). In general, PO_4^{3-} can also be adsorbed in the form of a complex with the hydroxides, which depends on the sacrificial anodic material. This is reflected in the production of sludge that can be removed by sedimentation and flocculation.

The increase of pH to 6.88 in the Zn system, promotes the formation of: Zn^{2+}, $Zn_3(PO_4)_2.4H_2O$(s), $ZnOH^+$, $ZnSO_4$ [118], and $Zn_4(OH)_6SO_4$[119], as shown in Fig. 8c. The reactions occurring in this system are 13,15–16 and 26–27,

$$Zn^{2+} + SO_4^{2-} \leftrightarrow ZnSO_4 \quad (26)$$

$$Zn(OH)_2 + 3Zn^{2+} + 4HO^- + SO_4^{2-} \rightarrow Zn_4(OH)_6SO_4 \quad (27)$$

The species showed in the Eqs. (18–27) were proposed in agreement with the equilibrium diagrams and initial and final concentrations of different ions, supported through diverse works reported.

The sludge content was determined for each system Al, Cu and Zn that produced 1.31, 1.15 and 0.41 g/L of sludge, per treatment [120].

3.8. Operating cost of the EC process

The operating costs in this work were calculated by Eq. (6), for each electrical material at its best conditions. The calculations were made based on the quantity of electricity that has passed through the electrochemical cell [121] and the results are summarized in Table 3. It is worth clarifying, that these costs are actually savings since the energy was supplied by a deep cycle battery, whose CD was controlled by a current regulator. The deep cycle battery was charged by a solar panel.

Table 3
Operating costs and Faradaic efficiency.

Electrode material	Costs		Theoretical concentration of the sacrificial anode	Faradaic efficiency (%)
	Units			
	kwh/L	Cent (US)/L	mg/L	
Aluminum	0.0044	0.0176	138	77.1
Zinc	0.0003	0.0012	100	198.6
Copper	0.0037	0.0148	486	54.7

Thus, the supplied solar irradiation was a function of the site where the experiment was conducted, while the instantaneous solar irradiation was observed to vary with the meteorological conditions: roughly, sunny or cloudy [122]. Average solar radiation was obtained from the values of NASA [123]. This work was carried out with the following coordinates: 19.399, − 99.714. The program estimated the value of 5.46 kWh/m^2/day.

Faradaic efficiency (FE) was calculated with Eq. (28) [124] where *C (measured)* is equal to the metal measured concentration in the bulk solution divided by *C(faraday)* that is the theoretical concentration calculated by Faraday's law (Eq. 5). A FE close to 1 means optimum system performance. Through this Equation, it is shown that the Zinc electrode gives off almost twice the theoretical amount, because the solid phase is always in equilibrium with the liquid phase with fast external mass transport [125]. This can be ascribed to the Zn oxidation with the simultaneous water reduction to produce hydrogen, applied current (*i*), and solution pH [71,126]. With the electrodes of Al and Cu, there was a FE> 100 because the applied current was diverted to secondary electrochemical reactions to proceed [127].

$$FE\% = (100)\left[\frac{C(measured)}{C(faraday)}\right] \tag{28}$$

According with the results observed in Table 3, FE is higher when the Zn electrodes are used at a current density of 0.356 mA/cm^2. This is because zinc hydroxides generate $ZnO_{(s)}$ (Eq. 29)[128]. This produces a layer on the anode, which may generate electro-oxidation as shown in Eq. 30, because ZnO has the capacity to function as photoanode [129]. Due to this, the sludge production is very small.

$$Zn(OH)_2 \rightarrow ZnO + H_2O \tag{29}$$

$$H_2O + ZnO \rightarrow ZnO(^{\cdot}OH) + H^+ + e^- \tag{30}$$

As current density increases, however, the FE decreases to 27.68% with a C(faraday) equal to 500 mg/L and a C(measured) equal to 138.4 mg/L.

3.9. Life Cycle Assessment

The LCI for the studied system under the three scenarios is summarized in Table 1S given as Supplementary material. To generate this LCI the FU of 1 L of treated wastewater was used.

For the environmental analysis of the different scenarios, all the inventory items presented in Table 3S were considered. Table 4S shows the assessed impact categories, and the identified hotspots in this study

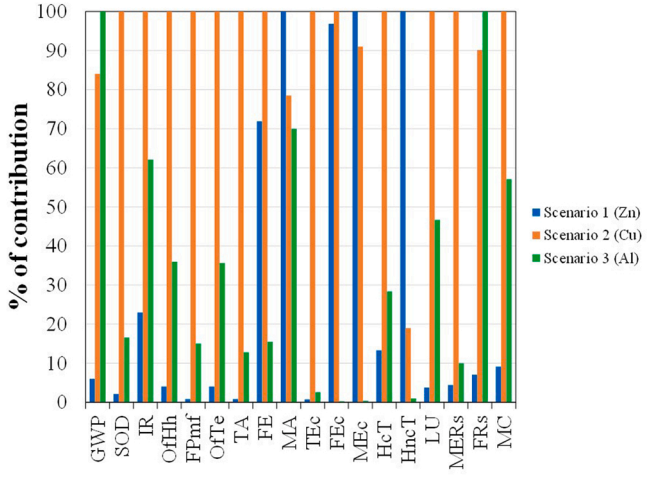

Fig. 12. Contribution analysis based on ReCiPe midpoint method characterization per functional unit for all scenarios: scenario 1 (Zn), scenario 2 (Cu) and scenario 3 (Al).

are terrestrial ecotoxicity by scenario 2 (Cu) (5.561 kg 1,4-DCB) and human non-carcinogenic toxicity by scenario 1(Zn), (1.642 kg 1,4-DCB). The toxicity potential is expressed in kg 1,4-dichlorobenzeneequivalents (1,4DCB-eq).

It can be seen in Fig. 12 that there is not a scenario that can be concluded as the best in terms of environmental impact in all categories. It is also important to note that the election of electrode material should not be made solely based on the performance of such material in the wastewater treatment. According to Fig. 12, nevertheless, Cu should not be elected as anodic material, not only because of its poor performance as electro-coagulant but also because exhibits the highest contribution to all midpoint categories excepting global warming. Regarding scenario 1, the use of Zn implies lower environmental impact than Al and Cu in most of the midpoint impact categories excepting for five of them, freshwater eutrophication, freshwater ecotoxicity, marine ecotoxicity and human carcinogenic and non-carcinogenic toxicity. These impact categories represent water quality and human health and they are the most frequently included in wastewater treatment LCAs [130].

The terrestrial ecotoxicity for scenario 2 (Cu) comes from anodic electrode material consumption derived from the electrode production (98.85%) and Na_2SO_4 (1.03%), mainly. The metal terrestrial ecotoxicity is an important impact influenced by the reactivity of the solid-phase metal pool. Copper is mainly associated with the variability in soil organic carbon and pH [131]. It is also considered that heavy metals can have several consequences in the human body such as cellular damages, carcinogenesis, neurotoxicity and might be the molecular basis for other noxious effects (Parkinson's disease and Alzheimer's disease) [132]. The agency for toxic substances and disease registry (ATSDR) has stated that the high levels of copper can cause harmful effects such as irritation of the nose, mouth and eyes, vomiting, diarrhea, stomach cramps, nausea, and even death [133].

The scenario 1(Zn) was less efficient than scenario 2(Cu) and scenario 3(Al) in the removal of COD, BOD5, and TOC. The human non-carcinogenic toxicity comes from final water emissions (99.64%) and anodic electrode material consumption (0.36%). The human health risk assessment is directly related to the degree of toxicity of heavy metals. The heavy metals as Zn, Cu, Cd, Cr, Pb, As, Cr, Mn, Fe and Ni have been associated with several non-carcinogenic related consequences [134]. In the case of Zinc, however, has a rather low toxicity and is an essential trace element for life. From the literature [135], there are very rare intoxication cases where Zn can be blamed. This suggests that the high % contribution to the aforementioned impact categories is due to the low efficiency removal in COD, color and turbidity, instead of the metal consumption.

Regarding the endpoint assessment, Table 4 summarizes the contribution in mPt to every damage category from every assessed scenario. It can be observed that in the category of human health, Scenario 1 (Zn) exhibits the highest contribution. Once again, this is the result of not achieving the same degree of removal efficiency than the other two anodes, especially in parameters like BOD_5, COD, TOC, total nitrogen and phosphates (see Table 1). Conversely, in the other two categories, scenario 1 (Zn) contribution is the lowest and scenario 2 (Cu) is the one with the highest % of contribution (see Fig. 13). It can be concluded then that, in this particular case, the damage to ecosystems and resources is exerted by the anode material and not by the water quality.

Al and Cu are two very well-known electrode materials used in

Table 4
Endpoint results from ReCiPe (H) for different anodic materials: scenario 1 (Zn), scenario 2 (Cu) and scenario 3 (Al). Impact factor score in millipoints (mPts).

Damage category	Unit	Scenario 1 (Zn)	Scenario 2 (Cu)	Scenario 3 (Al)
Human health	mPt	6.38	4.48	0.76
Ecosystems	mPt	0.03	0.20	0.05
Resources	mPt	3.91E-03	1.01E-02	6.17E-03
TOTAL	mPt	6.41	4.68	0.81

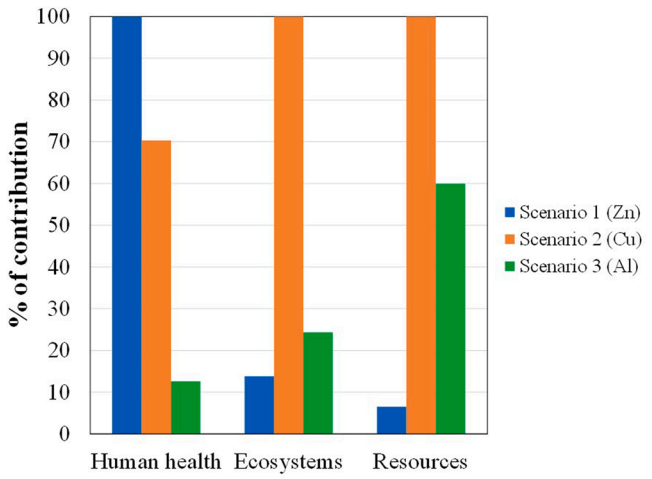

Fig. 13. ReCiPe end point impact categories for electrocoagulation system for the treatment of wastewater from a chocolate factory with three anodic materials: scenario 1 (Zn), scenario 2 (Cu) and scenario 3 (Al).

electrocoagulation and their use has been widely reported in the literature, albeit under different physicochemical characteristics of the wastewater. On the other hand, Zn has been reported to remove metallic ions by a similar mechanism than coagulation, and therefore appears as an interesting material worthy to be investigated as coagulant.

A sensibility and uncertainty analysis was conducted. The results were included in the manuscript as follows,

3.10. Sensibility analysis

Based on ISO 14044 (2018)[136] the sensibility analysis was conducted by varying the input and output data + 25% and − 25%, regarding anodic electrodes consumption, utilized chemicals, energy consumption and emissions to water bodies. The response was the end-point environmental impacts, i.e. human health, ecosystems and resources. The results are shown in Fig. 14 and it can be observed that the data increase or decrease proportionally to the applied variation. These data are used to establish the sensibility ratio (SR), which is calculated as follows,

$$SR = \frac{\%\Delta mPt_c}{\%\Delta mPt_v}$$

where $\%\Delta mPt_c$ is the percentage of variation in the calculated millipoints and $\%\Delta mPt_v$ is the percentage of millipoints variation when the increase or decrease of 25% is applied to the inventory data. The calculated SR for each scenario is shown in Table 1. It can be observed in the SR values reported in Table 5, that this ratio is one for Scenario 1(Zn) and Scenario 3(Al), which means that these data are not sensible to a variation of the inventory in the range of − 25% and + 25%. In the case of Scenario 2 (Cu), the SR was higher than 1: 1.25, 1.02 and 1.06 for human health, ecosystems and resources, respectively. In addition, there are in Table 5 the values for the percentage of standard deviation, which all of them are below 10%. This means that the processed data are sensible but not significant [137].

3.11. Uncertainty analysis

This analysis is helpful to establish the probability distribution of the input and output variables when applying the standard deviation for each scenario with the end-point model. This was conducted by the MonteCarlo method with the SimaPro software. For the simulation, 10,000 runs were considered to assess the toxicity of the scenarios with the probability distribution of chemical products, energy consumption and emission to water bodies. Fig. 15 shows the uncertainty analysis results and it is observed that the category with the highest results uncertainty is human health with scenario 2 (Cu), which is depicted by the length of the bars in a normal distribution with a confidence interval of 95%.

It is worth pointing out that within literature [138], the end point models are more relevant for decision making, although also pose a higher degree of uncertainty than the midpoint models.

4. Conclusions

The effect of anodic material (Al, Cu and Zn) on the removal efficiency of various physicochemical parameters was assessed in the treatment of a wastewater from a chocolate manufacturing industry by a solar-photovoltaic electrocoagulation system, within a relatively low current density range (0.356–1.781 mA/cm^2).

The best results were obtained with an initial pH of 4.38 and a density current of 1.781 mA/cm^2. Thus, the following results were obtained at these conditions.

The aluminum-based system exhibited the best results in terms of organic parameters. The achieved COD removal was 50% and BOD was 39%. The BI was increased from 0.49 to 0.59. TOC was diminished only 26.65%.

The copper-based system also showed a promising behaviour in the organics removal: 43% COD, 53% BOD, 30.7% TOC and the BI was 0.4.

The zinc-based system was slightly less efficient than the Cu and Al systems. The removal achieved were 39% COD, 30% BOD5, and 19% TOC. The BI increased from 0.49 to 0.56, improving the biodegradability of the treated wastewater. Color and turbidity removal were 89.5% and 73.86%, respectively. The electricity consumption is nil because solar energy was used.

The pH affects the removal of the assessed parameters. This removal is favored at the natural initial pH of the treated wastewater in the Al and Cu-based systems. The Zn-based system efficiency is not affected by initial pH in the investigated pH range (4−7).

The total solids were removed in a 67%, 50% and 42% in the following order as function of anodic material: Zn>Al>Cu.

The EC with any of the assessed metals can also be applied for disinfection purposes since the 99.98% of faecal and total coliforms was removed with any of the studied systems.

A mathematical model that well represents the evolution of COD and color with time was obtained and this can be used for comparison purposes and/or for the scaling-up of the process.

Regarding the life cycle assessment (LCA), it was concluded that the midpoint and endpoint environmental impacts are affected by both, the type of anodic material and by the quality of the water at the end of treatment. The treatment conducted with Cu as anodic material provided the highest % of contribution to all midpoint and endpoint categories, excepting global warming (GW), marine ecotoxicity (MEc), human non-carcinogenic toxicity (HncT), fossil resources scarcity (FRs) and human health damage (HHD). Therefore, the use of Cu as electrocoagulant for this process is not recommended. The use of Zn implies lower environmental impacts than Al and Cu in most of the mid and endpoint impact categories excepting for MEc, HncT and HH. This should be taken into account at the time of selecting the anodic material to conduct the electrocoagulation of wastewater.

The EC using solar panel and with Al electrodes, is a good option as pre-treatment of wastewater in the chocolate industry and can be conducted at larger scale.

CRediT authorship contribution statement

Violeta García Orozco (VGO), Ivonne Linares-Hernández (ILH) and Patricia Balderas Hernandez (PBH), Reyna Natividad (RN) and Claudia Alanis-Ramírez, acquired and analyzed the data. VGO and Carlos Barrera (CB) drafted the manuscript. Gabriela Roa (GR), RN and ILH

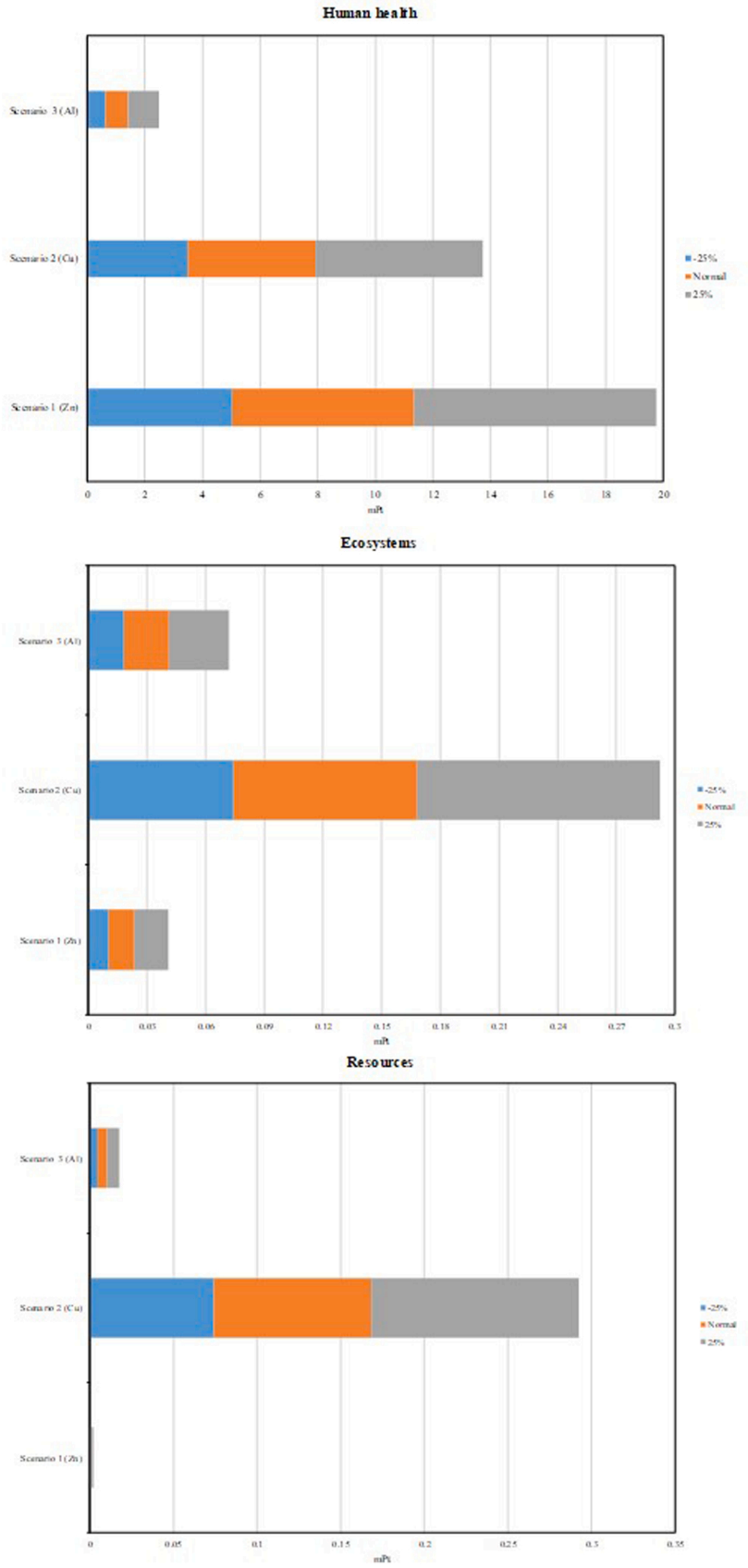

Fig. 14. Sensibility analysis of scenario 1 (Zn), scenario 2 (Cu) and scenario 3 (Al), a) Human Health, b) Ecosystems and c) Resources.

Table 5
Sensibility ratio and standard deviation percentage of end point impacts for scenario 1(Zn), scenario 2 (Cu) and scenario 3 (Al).

Damage category		Human health			Ecosystems			Resources		
		SR			SR			SR		
Scenario		1 (Zn)	2 (Cu)	3 (Al)	1 (Zn)	2 (Cu)	3 (Al)	1 (Zn)	2 (Cu)	3 (Al)
Yield variation %	**-25%**	1	1.08	1.01	1	1.07	1.01	1	1.06	1.01
	25%	1	1.25	1	1	0.96	1	1	0.97	1
%SD		1%	1%	1%	1%	1%	1%	1%	1%	1%

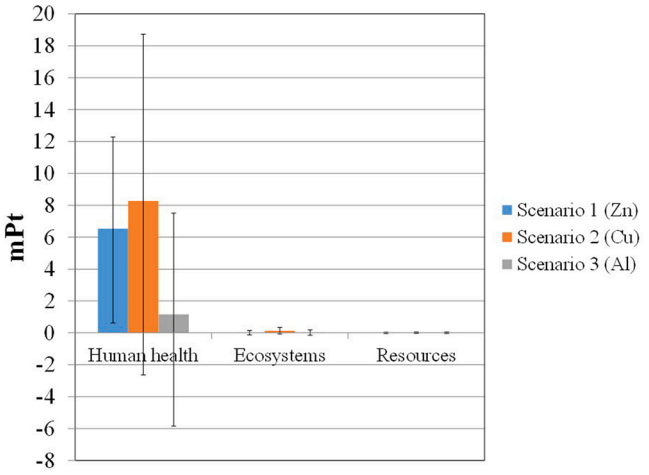

Fig. 15. Uncertainty analysis results for scenario 1 (Zn), scenario 2 (Cu) and scenario 3 (Al), ReCiPe 2016 Endpoint (H) V1.06 / World (2010) H/A confidence interval: 95%.

conceptualized and designed the study, revised the manuscript critically for important intellectual content. All authors approved the version of the manuscript to be published.

Declaration of Competing Interest

The authors declare that they have no known competing financial interests or personal relationships that could have appeared to influence the work reported in this paper.

Acknowledgments

V. Garcia is grateful to COMECYT, for the financial support through chair CAT-0125. The financial support of Universidad Autómoma Del Estado de México through project 6484/2021CIB is also acknowledged. The authors are also grateful to Autonomous University of Campeche for the analysis of SEM-EDS. Authors would also like to thank Dr. Ildefonso Esteban Pech Pech, M. Yolanda Espinosa Morales, M. Lizbeth Triana Cruz and M. Melina Tapia Tapia for the analysis of FTIR spectra. The technical support of Citlalit Martínez is also acknowledged.

Appendix A. Supporting information

Supplementary data associated with this article can be found in the online version at doi:10.1016/j.jece.2022.107969.

References

[1] A. Konstantas, H.K. Jeswani, L. Stamford, A. Azapagic, Environmental impacts of chocolate production and consumption in the UK, Food Res. Int. 106 (2018) 1012–1025, https://doi.org/10.1016/j.foodres.2018.02.042.
[2] F. Recanati, D. Marveggio, G. Dotelli, From beans to bar: a life cycle assessment towards sustainable chocolate supply chain, Sci. Total Environ. 613–614 (2018) 1013–1023, https://doi.org/10.1016/j.scitotenv.2017.09.187.
[3] Y. Jin, S. Kang, D. Hee, Y. Jin, W. Ri, Y. Min, et al., Calorie reduction of chocolate ganache through substitution of whipped cream, . J Ethn. Foods 4 (2017) 51–57, https://doi.org/10.1016/j.jef.2017.02.002.
[4] H.K. Khuntia, N. Janardhana, H.N. Chanakya, Fractionation of FOG (fat, oil, grease), wastewater and particulate solids based on low-temperature solidification and stirring, J. Water Process Eng. 34 (2020), 101167, https://doi.org/10.1016/j.jwpe.2020.101167.
[5] M. Kindlein, E. Elts, H. Briesen, Phospholipids in chocolate: structural insights and mechanistic explanations of rheological behavior by coarse-grained molecular dynamics simulations, J. Food Eng. (2018), https://doi.org/10.1016/j.jfoodeng.2018.02.014.
[6] I. Magalhães, L.D.F. Vilela, C. Santos, N. Lima, R.F. Schwan, Volatile compounds and protein profiles analyses of fermented cocoa beans and chocolates from different hybrids cultivated in Brazil, Food Res. Int. (2018), https://doi.org/10.1016/j.foodres.2018.04.012.
[7] S.A. Patil, V.P. Surakasi, S. Koul, S. Ijmulwar, A. Vivek, Y.S. Shouche, et al., Electricity generation using chocolate industry wastewater and its treatment in activated sludge based microbial fuel cell and analysis of developed microbial community in the anode chamber, Bioresour. Technol. 100 (2009) 5132–5139, https://doi.org/10.1016/j.biortech.2009.05.041.
[8] O.S. Toker, N. Konar, I. Palabiyik, H.R. Pirouzian, S. Oba, D.G. Polat, et al., Formulation of dark chocolate as a carrier to deliver eicosapentaenoic and docosahexaenoic acids: effects on product quality, Food Chem. (2018), https://doi.org/10.1016/j.foodchem.2018.02.019.
[9] G.Z. Kyzas, K.A. Matis, Electroflotation process: a review, J. Mol. Liq. 220 (2016) 657–664, https://doi.org/10.1016/j.molliq.2016.04.128.
[10] E. GilPavas, I. Dobrosz-Gómez, M.Á. Gómez-García, Optimization of sequential chemical coagulation - electro-oxidation process for the treatment of an industrial textile wastewater, J. Water Process Eng. 22 (2018) 73–79, https://doi.org/10.1016/j.jwpe.2018.01.005.
[11] S.M. Safwat, Treatment of real printing wastewater using electrocoagulation process with titanium and zinc electrodes, J Water Process Eng. 34 (2020), 101137, https://doi.org/10.1016/j.jwpe.2020.101137.
[12] I. Gajda, A. Stinchcombe, J. Greenman, C. Melhuish, I. Ieropoulos, Microbial fuel cell – a novel self-powered wastewater electrolyser for electrocoagulation of heavy metals, Int. J. Hydrog. Energy 42 (2017) 1813–1819, https://doi.org/10.1016/j.ijhydene.2016.06.161.
[13] E.S.Z. El-Ashtoukhy, N.K. Amin, Y.O. Fouad, H.A. Hamad, Intensification of a new electrocoagulation system characterized by minimum energy consumption and maximum removal efficiency of heavy metals from simulated wastewater, Chem. Eng. Process - Process Intensif. 154 (2020), 108026, https://doi.org/10.1016/j.cep.2020.108026.
[14] T. Kim, T. Kim, K. Zoh, Removal mechanism of heavy metal (Cu, Ni, Zn, and Cr) in the presence of cyanide during electrocoagulation using Fe and Al electrodes, J. Water Process Eng. 33 (2020), 101109, https://doi.org/10.1016/j.jwpe.2019.101109.
[15] M. Dolati, A.A. Aghapour, H. Khorsandi, S. Karimzade, Boron removal from aqueous solutions by electrocoagulation at low concentrations, J. Environ. Chem. Eng. 5 (2017) 5150–5156, https://doi.org/10.1016/j.jece.2017.09.055.
[16] P. Myllymäki, R. Lahti, H. Romar, U. Lassi, Removal of total organic carbon from peat solution by hybrid method—electrocoagulation combined with adsorption, J. Water Process Eng. 24 (2018) 56–62, https://doi.org/10.1016/j.jwpe.2018.05.008.
[17] A. Mohammadi, A. Khadir, R.M.A. Tehrani, Engineering optimization of nitrogen removal from an anaerobic digester e ffl uent by electrocoagulation process, J. Environ. Chem. Eng. 7 (2019), 103195, https://doi.org/10.1016/j.jece.2019.103195.
[18] M. Chen, O. Dollar, K. Shafer-Peltier, S. Randtke, S. Waseem, E. Peltier, Boron removal by electrocoagulation: removal mechanism, adsorption models and factors influencing removal, Water Res 170 (2020), 115362, https://doi.org/10.1016/j.watres.2019.115362.
[19] P.I. Omwene, M. Kobya, O.T. Can, Phosphorus removal from domestic wastewater in electrocoagulation reactor using aluminium and iron plate hybrid anodes, Ecol. Eng. 123 (2018) 65–73, https://doi.org/10.1016/j.ecoleng.2018.08.025.
[20] L. Xu, Q. Huang, X. Xu, G. Cao, C. He, Y. Wang, et al., Simultaneous removal of Zn2+ and Mn2+ ions from synthetic and real smelting wastewater using electrocoagulation process: influence of pulse current parameters and anions, Sep Purif. Technol. 188 (2017) 316–328, https://doi.org/10.1016/j.seppur.2017.07.036.
[21] Ö. Hanay, H. Hasar, Effect of anions on removing Cu2+, Mn2+ and Zn2+ in electrocoagulation process using aluminum electrodes, J. Hazard Mater. 189 (2011), https://doi.org/10.1016/j.jhazmat.2011.02.073.

[22] Y. Wang, H. Lin, F. Jin, J. Niu, J. Zhao, Y. Bi, et al., Electrocoagulation mechanism of perfluorooctanoate (PFOA) on a zinc anode: influence of cathodes and anions, Sci. Total Environ. 557–558 (2016) 542–550, https://doi.org/10.1016/j.scitotenv.2016.03.114.

[23] S. Kumari, R.N. Kumar, River water treatment using electrocoagulation for removal of acetaminophen and natural organic matter, Chemosphere 273 (2021), 128571, https://doi.org/10.1016/j.chemosphere.2020.128571.

[24] E.M. Nigri, A.L.A. Santos, S.D.F. Rocha, Removal of organic compounds, calcium and strontium from petroleum industry effluent by simultaneous electrocoagulation and adsorption, J. Water Process Eng. 37 (2020), 101442, https://doi.org/10.1016/j.jwpe.2020.101442.

[25] J. Esther Baby, I. Jaambavi, G. Rajeswari, T. Akshaya, Optimization removal of colour and organic solid pollutants from textile industry wastewater by electrocoagulation, Mater. Today Proc. (2021) 3–6, https://doi.org/10.1016/j.matpr.2021.03.339.

[26] T.S. Arturi, C.J. Seijas, G.L. Bianchi, A comparative study on the treatment of gelatin production plant wastewater using electrocoagulation and chemical coagulation, Heliyon 5 (2019), e01738, https://doi.org/10.1016/j.heliyon.2019.e01738.

[27] N. Lakshmi Kruthika, S. Karthika, G. Bhaskar Raju, S. Prabhakar, Efficacy of electrocoagulation and electrooxidation for the purification of wastewater generated from gelatin production plant, J. Environ. Chem. Eng. 1 (2013) 183–188, https://doi.org/10.1016/j.jece.2013.04.017.

[28] J.P. Maree, C.G.B. Cole, A. Gerber, J.L. Barnard, Treatment of gelatine factory effluent, Water SA 16 (1990) 265–268.

[29] M. Kobya, H. Hiz, E. Senturk, C. Aydiner, E. Demirbas, Treatment of potato chips manufacturing wastewater by electrocoagulation, Desalination 190 (2006) 201–211, https://doi.org/10.1016/j.desal.2005.10.006.

[30] Hermida L. Sudibyo, Suwardi. Application of Taguchi optimization on the cassava starch wastewater electrocoagulation using batch recycle method, AIP Conf. Proc. (2017) 1904, https://doi.org/10.1063/1.5011863.

[31] E. Bazrafshan, H. Moein, F. Kord Mostafapour, S. Nakhaie, Application of electrocoagulation process for dairy wastewater treatment, J. Chem. 2013 (2013) 7–10, https://doi.org/10.1155/2013/640139.

[32] S. Visigalli, M.G. Barberis, A. Turolla, R. Canziani, M. Berden Zrimec, R. Reinhardt, et al., Electrocoagulation–flotation (ECF) for microalgae harvesting – a review, Sep Purif. Technol. 271 (2021), 118684, https://doi.org/10.1016/j.seppur.2021.118684.

[33] Lubis M.R. Darmadi, Hizir, A. Chairunnisak, B. Arifin, Comparison of palm oil mill effluent electrocoagulation by using fe-fe and al-al electrodes: box-behnken design, ASEAN J. Chem. Eng. 18 (2018) 30–43, https://doi.org/10.29037/ajche.v1i0.559.

[34] M. Kobya, S. Delipinar, Treatment of the baker's yeast wastewater by electrocoagulation, J. Hazard Mater. 154 (2008) 1133–1140, https://doi.org/10.1016/j.jhazmat.2007.11.019.

[35] G. Roa-Morales, E. Campos-Medina, J. Aguilera-Cotero, B. Bilyeu, C. Barrera-Díaz, Aluminum electrocoagulation with peroxide applied to wastewater from pasta and cookie processing, Sep Purif. Technol. 54 (2007) 124–129, https://doi.org/10.1016/j.seppur.2006.08.025.

[36] M. Kobya, S. Delipinar, Treatment of the baker's yeast wastewater by electrocoagulation, J. Hazard Mater. 154 (2008) 1133–1140, https://doi.org/10.1016/j.jhazmat.2007.11.019.

[37] C. Tsioptsias, D. Petridis, N. Athanasakis, I. Lemonidis, A. Deligiannis, P. Samaras, Post-treatment of molasses wastewater by electrocoagulation and process optimization through response surface analysis, J. Environ. Manag. 164 (2015) 104–113, https://doi.org/10.1016/j.jenvman.2015.09.007.

[38] X. Li, T. Li, F. Zhang, Removal of caramel pigment from sauce wastewater by electrocoagulation process using aluminum electrodes, Appl. Mech. Mater. 261–262 (2013) 856–861, https://doi.org/10.4028/www.scientific.net/AMM.260-261.856.

[39] D. Valero, J.M. Ortiz, V. García, E. Expósito, V. Montiel, A. Aldaz, Electrocoagulation of wastewater from almond industry, Chemosphere 84 (2011) 1290–1295, https://doi.org/10.1016/j.chemosphere.2011.05.032.

[40] V.M. García-Orozco, G. Roa-Morales, I. Linares-Hernández, I.J. Serrano-Jimenes, M.A. Salgado-Catarino, R. Natividad, Electrocoagulation of a chocolate industry wastewater in a Downflow column electrochemical reactor, J. Water Process Eng. 42 (2021), 102057, https://doi.org/10.1016/j.jwpe.2021.102057.

[41] M. Amarine, B. Lekhlif, M. Sinan, A. El, J. Echaabi, Groundwater for Sustainable Development, Treat. Nitrate Rich. Groundw. Using Electro Alum. anodes. Ground Sustain Dev. 11 (2020), 100371, https://doi.org/10.1016/j.gsd.2020.100371.

[42] L.P. Zini, M. Longhi, E. Jonko, M. Giovanela, Treatment of automotive industry wastewater by electrocoagulation using commercial aluminum electrodes, Process Saf. Environ. Prot. (2020), https://doi.org/10.1016/j.psep.2020.06.029.

[43] J. Trompette, J. Lahitte, Effects of some ion-specific properties in the electrocoagulation process with aluminum electrodes, Colloids Surf. A Physicochem Eng. Asp. 629 (2021), 127507, https://doi.org/10.1016/j.colsurfa.2021.127507.

[44] A.A. Moneer, N.M. El-mallah, M.M. El-sadaawy, M. Khedawy, M.S.H. Ramadan, Kinetics, thermodynamics, isotherm modeling for removal of reactive Red 35 and disperse yellow 56 dyes using batch bi-polar aluminum electrocoagulation, Alex. Eng. J. 60 (2021) 4139–4154, https://doi.org/10.1016/j.aej.2021.02.061.

[45] Kalivel P., Jagadeesh T., Kavitha S., Padmanabhan D., Palanichamy J., Murphy A. Materials Today: Proceedings Comparative study on removal of yellow 10gw dye from aqueous solution using Al, Cu electrodes in electrocoagulation. Mater Today Proc 2020. https://doi.org/10.1016/j.matpr.2020.10.561.

[46] M. Kobya, P. Isaac, S. Mohammadzadeh, S. Yildirim, Z. Ukundimana, Phosphorous removal from anaerobically digested municipal sludge centrate by an electrocoagulation reactor using metal (Al, Fe and Al-Fe) scrap anodes, Process Saf. Environ. Prot. 152 (2021) 188–200, https://doi.org/10.1016/j.psep.2021.06.003.

[47] M. Kim, T. Kim, T. Kim, S. Joo, K. Zoh, Degradation mechanism of perfluorooctanoic acid (PFOA) during electrocoagulation using Fe electrode, Sep Purif. Technol. 247 (2020), 116911, https://doi.org/10.1016/j.seppur.2020.116911.

[48] A. Dura, C.B. Breslin, Electrocoagulation using stainless steel anodes: simultaneous removal of phosphates, Orange II and zinc ions, J. Hazard Mater. 374 (2019) 152–158, https://doi.org/10.1016/j.jhazmat.2019.04.032.

[49] Ghimire U., Jang M., Jung SP, Park D., Park SJ, Yu H., et al. Electrochemical Removal of Ammonium Nitrogen and COD of Domestic Wastewater using Platinum Coated Titanium as an Anode Electrode n.d. https://doi.org/10.3390/en12050883.

[50] S.M. Safwat, M.E. Matta, Performance evaluation of electrocoagulation process using zinc electrodes for removal of urea, Sep Sci. Technol. 0 (2019) 1–10, https://doi.org/10.1080/01496395.2019.1636067.

[51] F. Hussin, F. Abnisa, G. Issabayeva, M.K. Aroua, Removal of lead by solar-photovoltaic electrocoagulation using novel perforated zinc electrode, J. Clean. Prod. 147 (2017) 206–216, https://doi.org/10.1016/j.jclepro.2017.01.096.

[52] M. Esparza-Soto, O. Arzate-Archundia, C. Solís-Morelos, C. Fall, Treatment of a chocolate industry wastewater in a pilot-scale low-temperature UASB reactor operated at short hydraulic and sludge retention time, Water Sci. Technol. 67 (2013) 1353–1361, https://doi.org/10.2166/wst.2013.010.

[53] S. Alcaraz-Ibarra, M.A. Mier-Quiroga, M. Esparza-Soto, M. Lucero-Chávez, C. Fall, Treatment of chocolate-processing industry wastewater in a low-temperature pilot-scale UASB: Reactor performance and in-situ biogas use for bioenergy recovery, Biomass Bioenergy (2020) 142, https://doi.org/10.1016/j.biombioe.2020.105786.

[54] M. Esparza Soto, C. Solís Morelos, J.J. Herná, Anaerobic treatment of a medium strength industrial wastewater at low-temperature and short hydraulic retention time: a pilot-scale experience, Water Sci. Technol. 64 (2011) 1629–1635, https://doi.org/10.2166/wst.2011.741.

[55] M. Esparza-Soto, A. Jacobo-López, M. Lucero-Chávez, C. Fall, Anaerobic treatment of chocolate-processing industry wastewater at different organic loading rates and temperatures, Water Sci. Technol. 79 (2019) 2251–2259, https://doi.org/10.2166/wst.2019.225.

[56] M.A. García-Morales, J.C.G. Juárez, S. Martínez-Gallegos, G. Roa-Morales, E. Peralta, E.M. Del Campo López, et al., Pretreatment of real wastewater from the chocolate manufacturing industry through an integrated process of electrocoagulation and sand filtration, Int J. Photo (2018) 2018, https://doi.org/10.1155/2018/2146751.

[57] A. Shahedi, A.K. Darban, F. Taghipour, A. Jamshidi-Zanjani, A review on industrial wastewater treatment via electrocoagulation processes, Curr. Opin. Electrochem 22 (2020) 154–169, https://doi.org/10.1016/j.coelec.2020.05.009.

[58] M.A. Ahangarnokolaei, P. Attarian, B. Ayati, H. Ganjidoust, L. Rizzo, Life cycle assessment of sequential and simultaneous combination of electrocoagulation and ozonation for textile wastewater treatment, J. Environ. Chem. Eng. 9 (2021), 106251, https://doi.org/10.1016/j.jece.2021.106251.

[59] V. Lopez-Grimau, B. Amante García, L. Canals Casals, Life cycle assessment for the selection of electrodes in the electrocoagulation of waste water of the paper industry, 21th Int. Congr. Proj. Manag. Eng. (2017) 1243–1252, https://doi.org/http://hdl.handle.net/2117/108772.

[60] E. Demirbas, M. Kobya, Operating cost and treatment of metalworking fluid wastewater by chemical coagulation and electrocoagulation processes, Process Saf. Environ. Prot. 105 (2017) 79–90, https://doi.org/10.1016/j.psep.2016.10.013.

[61] Y. Liu, X.M. Hu, Y. Zhao, J. Wang, M.X. Lu, F.H. Peng, et al., Removal of perfluorooctanoic acid in simulated and natural waters with different electrode materials by electrocoagulation, Chemosphere 201 (2018) 303–309, https://doi.org/10.1016/j.chemosphere.2018.02.129.

[62] Z. Qi, S. You, N. Ren, Wireless electrocoagulation in water treatment based on bipolar electrochemistry, Electro Acta 229 (2017) 96–101, https://doi.org/10.1016/j.electacta.2017.01.151.

[63] N. Fayad, T. Yehya, F. Audonnet, C. Vial, Preliminary purification of volatile fatty acids in a digestate from acidogenic fermentation by electrocoagulation, Sep Purif. Technol. (2017), https://doi.org/10.1016/j.seppur.2017.04.041.

[64] V.K. Sandhwar, B. Prasad, Terephthalic acid removal from aqueous solution by electrocoagulation and electro-Fenton methods: process optimization through response surface methodology, Process Saf. Environ. Prot. 107 (2017) 269–280, https://doi.org/10.1016/j.psep.2017.02.014.

[65] C. Ferrag, M. Noroozifar, A.R. Modarresi-Alam, K. Kerman, Encapsulation of poly (m-aminobenzodioxol)-Fe3O4superparamagnetic nanorods and iron (III) thiocyanate complex in hydrogel toward hybrid solar cells, J. Environ. Chem. Eng. 9 (2021), 105612, https://doi.org/10.1016/j.jece.2021.105612.

[66] M. Madi, M. Tahir, S. Tasleem, Advances in structural modification of perovskite semiconductors for visible light assisted photocatalytic CO_2 reduction to renewable solar fuels: a review, J. Environ. Chem. Eng. 9 (2021), 106264, https://doi.org/10.1016/j.jece.2021.106264.

[67] K. Dermentzis, D. Marmanis, A. Christoforidis, A. Moumtzakis, Photovoltaic electrocoagulation process for remediation of chromium plating wastewaters, Desalin. Water Treat. 56 (2015) 1413–1418, https://doi.org/10.1080/19443994.2014.950992.

[68] N.A. Rahman, A.A. Linus, A. Philip, E.E. Jihed, U.J. Gilan, N.K.M.F. Kumar, et al., Development of solar power system for Sarawak peat water continuous electrocoagulation treatment process, IOP Conf. Ser. Mater. Sci. Eng. 1101 (2021), 012039, https://doi.org/10.1088/1757-899x/1101/1/012039.

[69] D. Valero, J.M. Ortiz, E. Expósito, V. Montiel, A. Aldaz, Electrocoagulation of a synthetic textile effluent powered by photovoltaic energy without batteries: direct connection behaviour, Sol. Energy Mater. Sol. Cells 92 (2008) 291–297, https://doi.org/10.1016/j.solmat.2007.09.006.

[70] S. Zhang, J. Zhang, W. Wang, F. Li, X. Cheng, Removal of phosphate from landscape water using an electrocoagulation process powered directly by photovoltaic solar modules, Sol. Energy Mater. Sol. Cells 117 (2013) 73–80, https://doi.org/10.1016/j.solmat.2013.05.027.

[71] Pavón-silva TB, Romero-tehuitzil H., Munguia G., Huacuz-villamar J. Photovoltaic Energy-Assisted Electrocoagulation of a Synthetic Textile Effluent 2018;2018.

[72] B. Khemila, B. Merzouk, A. Chouder, R. Zidelkhir, J.P. Leclerc, F. Lapicque, Removal of a textile dye using photovoltaic electrocoagulation, Sustain Chem. Pharm. 7 (2018) 27–35, https://doi.org/10.1016/j.scp.2017.11.004.

[73] G. Sharma, J. Choi, H.K. Shon, S. Phuntsho, Solar-powered electrocoagulation system for water and wastewater treatment, Desalin. Water Treat. 32 (2011) 381–388, https://doi.org/10.5004/dwt.2011.2756.

[74] R. Elkacmi, O. Boudouch, A. Hasib, M. Bouzaid, M. Bennajah, Photovoltaic electrocoagulation treatment of olive mill wastewater using an external-loop airlift reactor, Sustain Chem. Pharm. 17 (2020), 100274, https://doi.org/10.1016/j.scp.2020.100274.

[75] S. Zhang, X. Yang, Q. Cheng, M. Wang, C. Hu, B. Chai, et al., Treatment of wastewater containing nickel by electrocoagulation process using photovoltaic energy, Environ. Eng. Sci. 35 (2018) 484–492, https://doi.org/10.1089/ees.2016.0621.

[76] A.R.M. Tones, E. Eyng, C.L. Zeferino, S. Ferreira, O. de, A.A. Alves, A. de, M. R. Fagundes-Klen, et al., Spectral deconvolution associated to the Gaussian fit as a tool for the optimization of photovoltaic electrocoagulation applied in the treatment of textile dyes, Sci. Total Environ. 713 (2020), 136301, https://doi.org/10.1016/j.scitotenv.2019.136301.

[77] R. Elkacmi, O. Boudouch, A. Hasib, M. Bouzaid, M. Bennajah, Photovoltaic electrocoagulation treatment of olive mill wastewater using an external-loop airlift reactor, Sustain Chem. Pharm. (2020) 17, https://doi.org/10.1016/j.scp.2020.100274.

[78] N. Patcharaprakiti, Water purification by solar powered electrocoagulation system, Iran. J. Energy Environ. 8 (2017) 224–229.

[79] N. Drouiche, S. Aoudj, H. Lounici, M. Drouiche, T. Ouslimane, N. Ghaffour, Fluoride removal from pretreated photovoltaic wastewater by electrocoagulation: an investigation of the effect of operational parameters, Procedia Eng. 33 (2012) 385–391, https://doi.org/10.1016/j.proeng.2012.01.1218.

[80] C.J. Nawarkar, V.D. Salkar, Solar powered Electrocoagulation system for municipal wastewater treatment, Fuel 237 (2019) 222–226, https://doi.org/10.1016/j.fuel.2018.09.140.

[81] M.P.M. Combatt, W.C.S. Amorim, E.M. d S. Brito, A.F. Cupertino, R.C. S. Mendonça, Pereira HA. Design of parallel plate electrocoagulation reactors supplied by photovoltaic system applied to water treatment, Comput. Electron Agric. (2020) 177, https://doi.org/10.1016/j.compag.2020.105676.

[82] N. Karnaningroem, D.R. Anggraeni, Study of life cycle assessment (LCA) on water treatment, IOP Conf. Ser. Earth Environ. Sci. 799 (2021) 1–11, https://doi.org/10.1088/1755-1315/799/1/012036.

[83] APHA/AWWA/WEF. Standard Methods for the Examination of Water and Wastewater. Stand Meth. 2012.

[84] Puigdomenech I. Hydrochemical Equilibrium Constants Database (MEDUSA), Royal Institute of Technology, Stockholm, Sweden. 1997.

[85] Paillet F., Barrau C., Escudi R., Trably E. ScienceDirect Inhibition by the ionic strength of hydrogen production from the organic fraction of municipal solid waste 2019:1–10. https://doi.org/10.1016/j.ijhydene.2019.08.019.

[86] B.K. Nandi, S. Patel, Effects of operational parameters on the removal of brilliant green dye from aqueous solutions by electrocoagulation, Arab J. Chem. 10 (2013) S2961–S2968, https://doi.org/10.1016/j.arabjc.2013.11.032.

[87] CFE (Comisión Federal de Electricidad) Consulta tu tarifa. 2019 n.d. https://app.cfe.mx/aplicaciones/ccfe/tarifas/tarifas/Tarifas_casa.asp?Tarifa=DACTAR1&anio=2018 (accessed May 19, 2020).

[88] V.M. Garcia Orozco, C.E. Barrera Diaz, G. Roa Morales, I. Linares Hernandez, A comparative electrochemical-ozone treatment for removal of phenolphthalein, J. Chem. (2016) 2016, https://doi.org/10.1155/2016/8105128.

[89] ISO 14040:2006. Gestión ambiental. Ánalisis de ciclo de vida. Principios y marco de referencia. México: 2007.

[90] ISO 14044. Environmental management — Life cycle assessment — Requirements and guidelines, 2006.

[91] Huijbregts M., Steinmann ZJN, Elshout PMFM, Stam G., Verones F., Vieira MDM, et al. ReCiPe 2016 - A harmonized life cycle impact assessment method at midpoint and endpoint level. Report I: Characterization. 2016.

[92] Eddy Metcalf, Wastewater Engineering: Treatment and Reuse, 1058, McGraw-Hill, 2013.

[93] A. Barhoumi, S. Ncib, A. Chibani, K. Brahmi, W. Bouguerra, E. Elaloui, Industrial Crops & Products High-rate humic acid removal from cellulose and paper industry wastewater by combining electrocoagulation process with adsorption onto granular activated carbon, Ind. Crop Prod. 140 (2019), 111715, https://doi.org/10.1016/j.indcrop.2019.111715.

[94] M. Priya, J. Jeyanthi, Removal of COD, oil and grease from automobile wash water effluent using electrocoagulation technique, Microchem J. 150 (2019), 104070, https://doi.org/10.1016/j.microc.2019.104070.

[95] S. Aksu, Electrochemical equilibria of copper in aqueous phosphoric acid solutions, J. Electrochem Soc. (2009) 156, https://doi.org/10.1149/1.3215996.

[96] Dowman EA. Conservation in Field Archaeology. ilustrada. Universidad de Virginia: 1970.

[97] C. Barrera Díaz, B. Frontana Uribe, B. Bilyeu, Removal of organic pollutants in industrial wastewater with an integrated system of copper electrocoagulation and electrogenerated H2O2, Chemosphere 105 (2014) 160–164, https://doi.org/10.1016/j.chemosphere.2014.01.026.

[98] K. Sardari, J. Askegaard, Y.H. Chiao, S. Darvishmanesh, M. Kamaz, S. R. Wickramasinghe, Electrocoagulation followed by ultrafiltration for treating poultry processing wastewater, J. Environ. Chem. Eng. 6 (2018) 4937–4944, https://doi.org/10.1016/j.jece.2018.07.022.

[99] K. Sardari, P. Fyfe, D. Lincicome, S.R. Wickramasinghe, Aluminum electrocoagulation followed by forward osmosis for treating hydraulic fracturing produced waters, Desalination 428 (2018) 172–181, https://doi.org/10.1016/j.desal.2017.11.030.

[100] M. Doerre, L. Hibbitts, G. Patrick, N. Akafuah, Advances in automotive conversion coatings during pretreatment of the body structure: a review, Coatings 8 (2018) 405, https://doi.org/10.3390/coatings8110405.

[101] S. Garcia-Segura, M.M.S.G. Eiband, J.V. de Melo, C.A. Martínez-Huitle, Electrocoagulation and advanced electrocoagulation processes: a general review about the fundamentals, emerging applications and its association with other technologies, J. Electro Chem. 801 (2017) 267–299, https://doi.org/10.1016/j.jelechem.2017.07.047.

[102] Y. Orita, M. Akizuki, Y. Oshima, Kinetic analysis of zinc oxide anisotropic growth in supercritical water, J. Supercrit. Fluids 154 (2019), 104609, https://doi.org/10.1016/j.supflu.2019.104609.

[103] K.S. Hashim, N. Jasim, A. Shaw, D. Phipps, P. Kot, A.W. Alattabi, et al., Electrocoagulation as a green technology for phosphate removal from river water, Sep Purif. Technol. 210 (2019) 135–144, https://doi.org/10.1016/j.seppur.2018.07.056.

[104] M.A. Mamelkina, R. Tuunila, M. Sillänpää, A. Häkkinen, Systematic study on sulfate removal from mining waters by electrocoagulation, Sep Purif. Technol. 216 (2019) 43–50, https://doi.org/10.1016/j.seppur.2019.01.056.

[105] B.M.B. Ensano, L. Borea, V. Naddeo, V. Belgiorno, M.D.G. de Luna, M. Balakrishnan, et al., Applicability of the electrocoagulation process in treating real municipal wastewater containing pharmaceutical active compounds, J. Hazard. Mater. (2018), https://doi.org/10.1016/j.jhazmat.2018.07.093.

[106] Pinheiro E., Bottrel SEC, Starling MCVM, Leão MMD, Amorim CC. Degradation of carbendazim in water via photo-Fenton in Raceway Pond Reactor: assessment of acute toxicity and transformation products 2018.

[107] C. Arat, E. Biçer, Electrochemical monitoring of decolorization of diazo dye evans blue by fenton process under anaerobic conditions: kinetics and optimization 1, Russ. J. Electrochem 51 (2015) 730–742, https://doi.org/10.1134/S1023193515080029.

[108] J.E.L. Villa, C.D. Pereira, S. Cadore, A novel, rapid and simple acid extraction for multielemental determination in chocolate bars, Microchem J. 121 (2015) 199–204, https://doi.org/10.1016/j.microc.2015.03.008.

[109] A. Oulebsir, T. Chaabane, S. Zaidi, K. Omine, V. Alonzo, A. Darchen, et al., Preparation of mesoporous alumina electro-generated by electrocoagulation in NaCl electrolyte and application in fluoride removal with consistent regenerations, Arab J. Chem. (2017), https://doi.org/10.1016/j.arabjc.2017.04.007.

[110] A. Hubdar, A. Maitlo, J. Lee, J.Y. Park, J. Kim, K. Kim, et al., An energy-efficient air-breathing cathode electrocoagulation approach for the treatment of arsenite in aquatic systems, J. Ind. Eng. Chem. (2019), https://doi.org/10.1016/j.jiec.2019.01.026.

[111] M. Elazzouzi, A. El Kasmi, K. Haboubi, M.S. Elyoubi, A novel electrocoagulation process using insulated edges of Al electrodes for enhancement of urban wastewater treatment: techno-economic study, Process Saf. Environ. Prot. 116 (2018) 506–515, https://doi.org/10.1016/j.psep.2018.03.006.

[112] M. Molano-mendoza, D. Donneys-victoria, N. Marriaga-cabrales, M. Angel, G. Li, F. Machuca-martínez, MethodsX Synthesis of Mg-Al layered double hydroxides by electrocoagulation, MethodsX 5 (2018) 915–923, https://doi.org/10.1016/j.mex.2018.07.019.

[113] O. Sahu, D.G. Rao, R. Gopal, A. Tiwari, D. Pal, Treatment of wastewater from sugarcane process industry by electrochemical and chemical process: aluminum (metal and salt), J Water. Process Eng. 17 (2017) 50–62, https://doi.org/10.1016/j.jwpe.2017.03.005.

[114] P. Aswathy, R. Gandhimathi, S.T. Ramesh, P.V. Nidheesh, Department of civil engineering, national institute of technology, tiruchirappalli, department of civil engineering, vimal jyothi engineering college, chemperi, kannur, Sep Purif. Technol. (2016), https://doi.org/10.1016/j.seppur.2016.01.001.

[115] Whitten KW, E. Davis R., Peck L., Stanley GG. Student Solutions Manual. 2013.

[116] Lobnig R.E., Frankenthal R.P., Siconolfi D.J., Sinclair J.D., Stratmann M. Mechanism of Atmospheric Corrosion of Copper in the Presence of Submicron Ammonium Sulfate Particles at 300 and 373 K 1994;141:2935–2941.

[117] F. Habashi, S.A. Mikhail, Reduction of binary sulfate mixtures containing CuSO4 by H2, Can. J. Chem. 54 (1976), https://doi.org/10.1139/v76-525.

[118] S. Koter, M. Kultys, B. Gilewicz-Łukasik, I. Koter, Modeling the transport of sulfuric acid and its sulfates (MgSO4, ZnSO4, Na2SO4) through an anion-exchange membrane, Desalination 342 (2014) 75–84, https://doi.org/10.1016/j.desal.2013.10.025.

[119] C. Qiao, L. Shen, L. Hao, X. Mu, J. Dong, W. Ke, et al., Corrosion kinetics and patina evolution of galvanized steel in a simulated coastal-industrial atmosphere, J. Mater. Sci. Technol. 35 (2019) 2345–2356, https://doi.org/10.1016/j.jmst.2019.05.039.
[120] F.U. Kac, M. Kobya, E. Gengec, Removal of humic acid by fixed-bed electrocoagulation reactor: studies on modelling, adsorption kinetics and HPSEC analyses, J. Electro Chem. 804 (2017) 199–211, https://doi.org/10.1016/j.jelechem.2017.10.009.
[121] D.G. Bassyouni, H.A. Hamad, E.-S.Z. El-Ashtoukhy, N.K. Amin, M.M.A. El-Latif, Comparative performance of anodic oxidation and electrocoagulation as clean processes for electrocatalytic degradation of diazo dye Acid Brown 14 in aqueous medium, J. Hazard. Mater. 335 (2017) 178–187, https://doi.org/10.1016/j.jhazmat.2017.04.045.
[122] C. Phalakornkule, T. Luanwuthi, P. Neragae, E.J. Moore, A continuous-flow sparged packed-bed electrocoagulator for dye decolorization, J. Taiwan Inst. Chem. Eng. 64 (2016) 124–133, https://doi.org/10.1016/j.jtice.2016.03.046.
[123] NASA (National Aeronautics and Space). POWER Data Access Viewer 2018. https://power.larc.nasa.gov/data-access-viewer/ (accessed May 19, 2020).
[124] A.S. Naje, S. Chelliapan, Z. Zakaria, M.A. Ajeel, K. Sopian, H.A. Hasan, Electrocoagulation by solar energy feed for textile wastewater treatment including mechanism and hydrogen production using a novel reactor design with a rotating anode, RSC Adv. 6 (2016) 10192–10204, https://doi.org/10.1039/C5RA26032A.
[125] Lukas Dubrawski K. (The U of BC. A Thesis submitted in partial fulfilment of the requirements for the degree. Columbia: 2013.
[126] C.M. Van Genuchten, K.N. Dalby, M. Ceccato, S.L.S. Stipp, K. Dideriksen, Factors affecting the Faradaic efficiency of Fe(0) electrocoagulation, J. Environ. Chem. Eng. 5 (2017) 4958–4968, https://doi.org/10.1016/j.jece.2017.09.008.
[127] S. Müller, T. Behrends, C.M. van Genuchten, Sustaining efficient production of aqueous iron during repeated operation of Fe(0)-electrocoagulation, Water Res. 155 (2019) 455–464, https://doi.org/10.1016/j.watres.2018.11.060.
[128] M. Kumar, C. Sasikumar, Electrodeposition of nanostructured ZnO thin film: a review, Am. J. Mater. Sci. Eng. 2 (2014) 18–23, https://doi.org/10.12691/ajmse-2-2-2.
[129] C.B. Ong, L.Y. Ng, A.W. Mohammad, A review of ZnO nanoparticles as solar photocatalysts: synthesis, mechanisms and applications, Renew. Sustain Energy Rev. 81 (2018) 536–551, https://doi.org/10.1016/j.rser.2017.08.020.
[130] S.M. Rahman, M.J. Eckelman, A. Onnis-Hayden, A.Z. Gu, Comparative life cycle assessment of advanced wastewater treatment processes for removal of chemicals of emerging concern, Environ. Sci. Technol. 52 (2018) 11346–11358, https://doi.org/10.1021/acs.est.8b00036.
[131] A. Liu, Q. Liao, M. Li, M. Li, Z. Meng, Q. Zhang, et al., The influence of aging on the comparative terrestrial ecotoxicity potential of copper and zinc in soils, Environ. Sci. Pollut. Res. 25 (2018) 28094–28101, https://doi.org/10.1007/s11356-018-2704-9.
[132] M. Jaishankar, T. Tseten, N. Anbalagan, B.B. Mathew, K.N. Beeregowda, Toxicity, mechanism and health effects of some heavy metals, Inter. Toxicol. 7 (2014) 60–72, https://doi.org/10.2478/intox-2014-0009.
[133] ATSDR. Toxicological Profile for Copper. 2004.
[134] Kabata-Pendias A., Pendias H. Trace Elements in Soils and Plants Third Edition. 2007.
[135] L.M. Plum, L. Rink, H. Haase, The essential toxin: impact of zinc on human health, Open Access Int. J. Environ. Res Public Heal 7 (2010) 7, https://doi.org/10.3390/ijerph7041342.
[136] DIN. DIN EN ISO 14044:2018–05 Environmental management - Life cycle. 2018.
[137] N. Karnaningroem, D.R. Anggraeni, Study of Life Cycle Assessment (LCA) on water treatment, IOP Conf. Ser. Earth Environ. Sci. (2021) 799, https://doi.org/10.1088/1755-1315/799/1/012036.
[138] UNEP. Evaluation of Environmental Impacts in Life Cycle Assessment. vol. 2. 2003. https://doi.org/10.1186/1758–5996-2–73.